IOPscience

The geometry of the limit of **N = 2** minimal models

The geometry of the limit of $N = 2$ minimal models

Stefan Fredenhagen and Cosimo Restuccia

Max-Planck-Institut für Gravitationsphysik, Albert-Einstein-Institut, Am Mühlenberg 1, D-14476 Golm, Germany

E-mail: Stefan.Fredenhagen@aei.mpg.de and Cosimo.Restuccia@aei.mpg.de

Abstract

We consider the limit of two-dimensional $N = (2, 2)$ superconformal minimal models when the central charge approaches $c = 3$. Starting from a geometric description as nonlinear sigma models, we show that one can obtain two different limit theories. One is the free theory of two bosons and two fermions, the other one is a continuous orbifold thereof. We substantiate this claim by detailed conformal field theory computations.

PACS numbers: 11.10.Kk, 11.25.Hf

1. Introduction

Sequences of two-dimensional conformal field theories and their limits have been analysed in [1–8]. The motivation to study them arises on the one hand, because one can use them to explore non-rational models that occur as limits of sequences of rational theories. On the other hand, the analysis of such sequences might shed light on the structure of the space of two-dimensional field theories. There are several ideas about what a good notion of distance on such a space would be, e.g., the Zamolodchikov metric [9, 10] or g-factors of conformal interfaces (for a recent discussion see [11]). If one has a notion of distance or more generally a topology, one can also discuss the question of convergence of sequences of theories. Conversely, lacking a proper understanding of theory space, one may study sequences of theories in order to learn more about what the right notion of convergence should be.

The study of limits of sequences of two-dimensional conformal field theories was pioneered in [1] for the limit of Virasoro minimal models when the central charge approaches $c = 1$. The general idea of that construction is to define fields in the limit theory as limits of averages of fields. More precisely, given a smooth, non-negative function $f(h)$ of fast enough decay that describes a certain averaging over conformal weights, the corresponding limit field Φ_f arises from weighted averages

$$\Phi_f^{(k)} = \sum_i f(h_i) \, \phi_i^{(k)} \tag{1.1}$$

of primary fields $\phi_i^{(k)}$ in the kth model with conformal weight h_i. Correlators of limit fields are then defined as limits of correlators of averaged fields. In order to obtain finite and sensible correlators in the limit, one can make use of the freedom to rescale fields and correlators and to redefine the fields $\phi_i^{(k)}$ by individual phases. A priori it is not guaranteed that in this way one arrives at a valid conformal field theory, but in all examples that have been studied over the years, the limit theory seems to be well behaved.

The above procedure is ambiguous when other quantum numbers are available, because there is some freedom of how to treat them while taking the limit. In the limit of $N = (2, 2)$ superconformal minimal models at central charge $c = 3$, which we explore here, we will encounter this ambiguity because of the presence of the $U(1)$ current J in the $N = 2$ superconformal algebra and the corresponding charge Q. On the one hand, we could keep the charge fixed in the limit and define field averages

$$^{(1)}\Phi_f^{(k)} = \sum_i f(h_i, Q_i)\,\phi_i^{(k)}, \tag{1.2}$$

corresponding to a certain test function $f(h, Q)$ by an obvious generalization of (1.1). This leads to the limit theory constructed in [8] with a continuous spectrum of charged primary fields. On the other hand, one could rescale the charges and define new averaged fields

$$^{(2)}\Phi_f^{(k)} = \sum_i f(h_i, Q_i(k + 2))\,\phi_i^{(k)}. \tag{1.3}$$

Because of the rescaling, in this theory the primary fields have charge zero, and we will show that this limit is equivalent to a free theory of two uncompactified bosons and two fermions. The discrete quantum number that arises from the rescaled charge of the primary fields is then interpreted as the eigenvalue of the rotation operator on the plane spanned by the two bosonic fields. In the process of defining the limit theory we will see that in addition to a global rescaling of the fields we also have to make use of the freedom to redefine the ingredient fields $\phi_i^{(k)}$ of $^{(2)}\Phi_f^{(k)}$ by individual phases compared to the conventions used for the ingredient fields in the definition of $^{(1)}\Phi_f^{(k)}$ in the other limit construction [8].

The appearance of two different limit theories can also be understood from a geometric point of view. The minimal models can be described by nonlinear sigma models [12] with a target space having the topology of a disc with infinite circumference but with a finite radius $\sqrt{\pi(k+2)/2}$, which goes to infinity in the limit $k \to \infty$. If one focuses on the region around the centre while taking the limit, the metric approaches the flat metric on the plane. This is the free limit theory described above. On the other hand, one could focus on the region close to the (singular) boundary of the disc. As explained in section 2, one can use T-duality to show that the corresponding limit theory should be given by a free theory of two bosons and two fermions orbifolded by the rotation group $SO(2)$. We will verify explicitly that this continuous orbifold coincides with the limit theory involving the fields $^{(1)}\Phi_f^{(k)}$ that was constructed in [8].

The plan of the paper is the following. We will start our analysis in section 2 by discussing the two possible limits starting from a geometric description. In section 3 we will confirm that the limit procedure using the fields $^{(2)}\Phi_f^{(k)}$ (see (1.3)) with rescaled charges leads to a free field theory; we determine the partition function, the three-point function and boundary conditions in the limit and compare them to the free field theory results. Thereafter in section 4 we show that the other limit theory involving the fields $^{(1)}\Phi_f^{(k)}$ (see (1.2)) is equivalent to a continuous orbifold by matching the partition function and boundary conditions, and we close in section 5 with a brief discussion.

2. The geometry of minimal models and the limit

In [12], Maldacena, Moore and Seiberg gave a geometric description of $N = (2, 2)$ minimal models in terms of a supersymmetric nonlinear sigma model on a two-dimensional target space with the topology of a disc and with the metric

$$\mathrm{d}s^2 = \frac{k+2}{1-\rho^2}(\mathrm{d}\rho^2 + \rho^2\mathrm{d}\varphi^2), \tag{2.1}$$

where the radial coordinate ρ runs from 0 to 1, and the angular coordinate φ is 2π-periodic. In addition there is a non-trivial dilaton field Φ of the form

$$\mathrm{e}^{\Phi(\rho,\varphi)-\Phi_0} = \frac{1}{\sqrt{1-\rho^2}}. \tag{2.2}$$

The geometry is such that the boundary at $\rho = 1$ is at a finite distance $\frac{\pi}{2}\sqrt{k+2}$ from the centre at $\rho = 0$, but the circumference of a circle at radius ρ is $2\pi\rho\sqrt{\frac{k+2}{1-\rho^2}}$, and it diverges as $\rho \to 1$.

Given the geometric interpretation, we now want to analyse what happens for large levels k. One way to take the geometric limit is to introduce a new coordinate

$$\rho' = \sqrt{k+2}\,\rho, \tag{2.3}$$

such that the metric reads

$$\mathrm{d}s^2 = \frac{1}{1-\rho'^2/(k+2)}(\mathrm{d}\rho'^2 + \rho'^2\mathrm{d}\varphi^2). \tag{2.4}$$

Keeping ρ' fixed while taking the limit $k \to \infty$ leads to the flat metric on the plane.

From this analysis one would like to conclude that the limit of $N = (2, 2)$ minimal models for $k \to \infty$ is a free theory. At first sight this is in conflict with the analysis in [8], where the limit of minimal models was shown to be a theory containing fields with a continuous $U(1)$ charge that should not be present in a free theory. This conflict can be resolved by comparing more carefully how the limits are taken in these two approaches.

In a minimal model of level k, Neveu–Schwarz primary fields $\phi_{l,m}$ are labelled by two integers satisfying $0 \leqslant l \leqslant k$, $|m| \leqslant l$ and $l + m$ even. In [8] the fields in the limit theory arise from fields $\phi_{l,m}$ where l and m grow linearly with k in the limit, while the difference $l - |m| =: 2n$ is kept fixed. To compare this procedure to the geometric limit we need a geometric interpretation of the fields $\phi_{l,m}$, which was also given in [12]. The fields $\phi_{l,m}$ correspond to wavefunctions

$$\psi_{l,m}(\rho, \varphi) = \rho^{|m|}\mathrm{e}^{im\varphi}{}_2F_1\left(\frac{|m|+l}{2} + 1, \frac{|m|-l}{2}; |m|+1; \rho^2\right), \tag{2.5}$$

which are eigenfunctions of the (dilaton-corrected) Laplacian,

$$\left(-\tfrac{1}{2}\nabla^2 + (\nabla\Phi)\cdot\nabla\right)\psi_{l,m}(\rho, \varphi) = 2h_{l,m}\,\psi_{l,m}(\rho, \varphi). \tag{2.6}$$

Here, $_2F_1$ is the hypergeometric function, and

$$h_{l,m} = \frac{l(l+2) - m^2}{4(k+2)} \tag{2.7}$$

is the conformal weight of the field $\phi_{l,m}$.

When we now take the geometric limit to the flat plane, the wavefunctions $\psi_{l,m}$ should approach the eigenfunctions of the flat Laplacian. In radial coordinates, these are given by

$$\psi_{p,m}^{\mathrm{flat}}(\rho', \varphi) = \mathrm{e}^{im\varphi}J_{|m|}(p\rho'), \tag{2.8}$$

where J is a Bessel function of the first kind. They satisfy

$$-\frac{1}{2}\nabla^2_{\text{flat}}\psi^{\text{flat}}_{p,m}(\rho',\varphi) = \frac{p^2}{2}\psi^{\text{flat}}_{p,m}(\rho',\varphi). \tag{2.9}$$

Comparing the angular dependence of $\psi_{l,m}$ and $\psi^{\text{flat}}_{p,m}$ one observes immediately that the label m should be kept fixed in the limit. For the eigenvalue $h_{l,m}$ to approach $h_p = \frac{p^2}{4}$, the label l has to grow with the square root of k, namely $l \approx p\sqrt{k+2}$. Then the wavefunctions $\psi_{l,m}$ behave as

$$(k+2)^{|m|/2}\psi_{l,m} = \rho'^{|m|}e^{im\varphi}\,_2F_1\left(\frac{|m|+l}{2}+1, \frac{|m|-l}{2}; |m|+1; \frac{\rho'^2}{k+2}\right) \tag{2.10}$$

$$= e^{im\varphi}\sum_{n=0}^{(l-|m|)/2}\frac{\left(\frac{l+|m|}{2}\right)_n\left(\frac{-l+|m|}{2}\right)_n}{n!(|m|+1)_n}(\rho')^{2n+|m|}(k+2)^{-n} \tag{2.11}$$

$$= e^{im\varphi}\sum_{n=0}^{(l-|m|)/2}\frac{(-1)^n}{n!(|m|+1)_n}\left(\frac{l-|m|-2n+2}{2\sqrt{k+2}}\right)\cdots\left(\frac{l-|m|}{2\sqrt{k+2}}\right)$$
$$\times\left(\frac{l+|m|}{2\sqrt{k+2}}\right)\cdots\left(\frac{l+|m|+2n-2}{2\sqrt{k+2}}\right)(\rho')^{2n+|m|} \tag{2.12}$$

$$\sim e^{im\varphi}\sum_{n=0}^{\infty}\frac{(-1)^n p^{2n} 2^{-2n}}{n!(|m|+1)_n}(\rho')^{2n+|m|} \tag{2.13}$$

$$\sim e^{im\varphi}J_{|m|}(p\rho'). \tag{2.14}$$

Thus up to an overall normalization factor the wavefunctions $\psi_{l,m}$ approach the wavefunctions of the free theory.

On the one hand, this suggests that there is a free field theory limit of minimal models by scaling $l \approx p\sqrt{k+2}$ and keeping m fixed. This will be examined further in section 3. On the other hand, this means that the limit theory found in [8] should correspond to a different way of taking the geometric limit. Indeed for fixed $l - |m| = 2n$ the wavefunction $\psi_{l,m}$ is, apart from the angular part, a polynomial in ρ containing $n+1$ terms with powers ranging from $\rho^{|m|}$ to $\rho^{|m|+2n}$. If $|m|$ is large, the wavefunctions are localized close to $\rho = 1$, in the region where the metric and the dilaton diverge and the sigma model description becomes singular, so that one cannot easily extract a sensible geometric interpretation. It was however observed in [12] that under a T-duality the minimal model is mapped to its own $\mathbb{Z}_{k+2}$ orbifold described by

$$d\tilde{s}^2 = \frac{k+2}{1-\tilde{\rho}^2}(d\tilde{\rho}^2 + \tilde{\rho}^2 d\tilde{\varphi}^2), \tag{2.15}$$

$$e^{\tilde{\Phi}-\Phi_0} = \frac{1}{\sqrt{k+2}}\frac{1}{\sqrt{1-\tilde{\rho}^2}}, \tag{2.16}$$

$$\tilde{\varphi} \equiv \tilde{\varphi} + \frac{2\pi}{k+2}. \tag{2.17}$$

T-duality maps the problematic region around $\rho = 1$ to the region close to the conical singularity of the orbifold at $\tilde{\rho} = 0$. This suggests that the limit of minimal models of [8] corresponds to taking the limit in the orbifolded model by focusing on the region around $\tilde{\rho} = 0$. By introducing again a rescaled variable $\tilde{\rho}' = \sqrt{k+2}\tilde{\rho}$ and keeping $\tilde{\rho}'$ fixed in the

limit, the metric $\mathrm{d}\tilde{s}^2$ approaches the flat metric on the plane. On the other hand, according to (2.17) all angles have to be identified. The resulting limit theory is thus the theory on a flat plane $\mathbb{R}^2$ orbifolded by the rotation group $SO(2)$.

In section 4 we will construct this orbifold conformal field theory and show that it precisely matches the limit theory of [8].

3. Free field limit

The geometric analysis of section 2 suggests that the $N = 2$ minimal models have a free field limit when the labels of the Neveu–Schwarz primary fields $\phi_{l,m}$ are treated such that $l \approx \sqrt{k+2}\, p$ and m stays fixed in the limit. As $m = -(k+2)Q$ for these fields, we are led to consider the limit of averaged fields ${}^{(2)}\Phi_f^{(k)}$ that uses a charge rescaled by $(k+2)$ (see (1.3)). We will first analyse the behaviour of the partition function in the limit. We will then turn to the actual construction of the fields in the limit theory, and determine the bulk three-point function and boundary conditions.

3.1. Partition function

We will now reproduce the partition function of the free theory of two uncompactified bosons and two fermions as the limit of the partition functions of minimal models. We focus on the Neveu–Schwarz sector, and for the minimal models we define

$$\mathcal{P}_k^{\mathrm{NS}}(\tau, \nu) = \mathrm{Tr}_{\mathcal{H}_k^{\mathrm{NS}}} \left(q^{L_0 - \frac{c}{24}} z^{J_0} \bar{q}^{\bar{L}_0 - \frac{c}{24}} \bar{z}^{\bar{J}_0} \right), \tag{3.1}$$

where J_0 is the zero mode of the $U(1)$ current of the $N = 2$ superconformal algebra, and $q = \mathrm{e}^{2\pi \mathrm{i}\tau}$ and $z = \mathrm{e}^{2\pi \mathrm{i}\nu}$. Note that $\mathcal{P}_k^{\mathrm{NS}}(\tau, \nu)$ does not depend holomorphically on τ and ν, but we suppress the dependence on $\bar{\tau}$ and $\bar{\nu}$ to shorten the notation. $\mathcal{H}_k^{\mathrm{NS}}$ is the full supersymmetric Hilbert space for the Neveu–Schwarz sector,

$$\mathcal{H}_k^{\mathrm{NS}} = \bigoplus_{0 \leqslant l \leqslant k} \bigoplus_{\substack{|m| \leqslant l \\ l+m \text{ even}}} \mathcal{H}_{l,m} \otimes \mathcal{H}_{l,m}, \tag{3.2}$$

and the Neveu–Schwarz spectrum of the actual minimal model corresponds to a (GSO-like) projection thereof. For $k \to \infty$ the partition function diverges: there are infinitely many states approaching the same conformal weight and charge. This can be seen by looking at the contribution of the Neveu–Schwarz ground states,

$$\mathcal{P}_k^{\mathrm{NS,g.s.}}(\tau, \nu) = \sum_{\substack{|m| \leqslant l \leqslant k \\ l+m \text{ even}}} (q\bar{q})^{\frac{(l+1)^2 - m^2}{4(k+2)}} (z\bar{z})^{-\frac{m}{k+2}}, \tag{3.3}$$

where we sum over the leading term of the minimal model characters given in equation (A.12). By introducing the summation variable $n = \frac{1}{2}(l - |m|)$, we can rewrite the sum and perform the summation over m,

$$\mathcal{P}_k^{\mathrm{NS,g.s.}}(\tau, \nu) = \sum_{n=0}^{\lfloor \frac{k}{2} \rfloor} (q\bar{q})^{\frac{(2n+1)^2}{4(k+2)}} \left(\sum_{m=0}^{k-2n} + \sum_{m=-k+2n}^{-1} \right) (q\bar{q})^{\frac{(2n+1)|m|}{2(k+2)}} (z\bar{z})^{-\frac{m}{k+2}} \tag{3.4}$$

$$= \sum_{n=0}^{\lfloor \frac{k}{2} \rfloor} (q\bar{q})^{\frac{(2n+1)^2}{4(k+2)}} \left[\frac{1 - (q\bar{q})^{\frac{2n+1}{2(k+2)}(k-2n+1)} (z\bar{z})^{-\frac{k-2n+1}{k+2}}}{1 - (q\bar{q})^{\frac{2n+1}{2(k+2)}} (z\bar{z})^{-\frac{1}{k+2}}} + \frac{1 - (q\bar{q})^{\frac{2n+1}{2(k+2)}(k-2n+1)} (z\bar{z})^{\frac{k-2n+1}{k+2}}}{1 - (q\bar{q})^{\frac{2n+1}{2(k+2)}} (z\bar{z})^{\frac{1}{k+2}}} \right]. \tag{3.5}$$

Here, $\lfloor x \rfloor$ denotes the greatest integer smaller or equal x. Now let us cut off the summation over n by $n \leqslant \Lambda\sqrt{k+2}$ with $0 < \Lambda < 1$. In this summation range, the denominators in (3.5) go to zero, and the summands diverge as $\frac{k+2}{n+\cdots}$. The sum over n produces a logarithmic divergence, such that the leading divergence of the partition function is of the form $(k+2)\log(k+2)$. The divergence signals an infinite degeneracy of states. Part of the divergence might be resolved by introducing additional quantum numbers that lift the degeneracy; on the other hand, there can be a divergence due to the emergence of a continuous spectrum, in which case we can regularize the partition function by rescaling the density of states appropriately[1].

The fields we are interested in have fixed label m, and their $U(1)$ charges $Q = -\frac{m}{k+2}$ (the eigenvalues of J_0) approach zero in the limit. To cure the divergence associated to the appearance of infinitely many chargeless fields, we want to keep track of the quantum number m in the limit. In the free field theory, m corresponds to the eigenvalue of the angular momentum operator M, and we could insert $\mathrm{e}^{\mathrm{i}\varphi M}$ in the partition function: in this way the partition function is written as a formal power series in $\mathrm{e}^{\mathrm{i}\varphi}$ and $\mathrm{e}^{-\mathrm{i}\varphi}$, and the coefficient of $\mathrm{e}^{\mathrm{i}m\varphi}$ gives the contribution of states of a given angular momentum m. In the geometric description of the minimal models, there is a $U(1)$ rotation symmetry in the classical theory, but it is broken to a $\mathbb{Z}_{k+2}$ symmetry in the quantum model. The rotation by an angle $2\pi\mathrm{i}\frac{r}{k+2}$ (r integer) is realized by the operator g^r, where g acts on states in $\mathcal{H}_{l,m} \otimes \mathcal{H}_{l,m}$ by multiplication with the phase $\mathrm{e}^{2\pi\mathrm{i}\frac{m}{k+2}}$. To mimic the insertion of $\mathrm{e}^{\mathrm{i}\varphi M}$ in the free field theory, we therefore introduce the operator $g^{\lfloor \frac{\varphi}{2\pi}(k+2)\rfloor}$ in the partition function, such that states with a given m will get the phase $\mathrm{e}^{\mathrm{i}m\varphi}$ in the limit.

The regularized partition function therefore becomes (we use standard conventions for ϑ-functions as summarized in appendix A)

$$\mathcal{P}^{\mathrm{NS}}_{k,(\varphi)}(\tau,\nu) = \left|\frac{\vartheta_3(\tau,\nu)}{\eta^3(\tau)}\right|^2 \sum_{m=-k}^{k} \mathrm{e}^{2\pi\mathrm{i}\frac{m}{k+2}\lfloor\frac{\varphi}{2\pi}(k+2)\rfloor}(z\bar{z})^{-\frac{m}{k+2}} \sum_{\substack{l=|m| \\ l+m\ \mathrm{even}}}^{k} (q\bar{q})^{\frac{(l+1)^2-m^2}{4(k+2)}} \left|\Gamma^{(k)}_{lm}(\tau,\nu)\right|^2,$$
(3.6)

where we used the minimal model characters given in equation (A.12). $\Gamma^{(k)}_{lm}$ is defined in equation (A.14), it is of the form

$$\Gamma^{(k)}_{lm} = 1 + (\text{subtractions from singular vectors}), \tag{3.7}$$

and its behaviour for large k is given in equation (A.17). The contribution of a fixed m is then

$$\mathcal{P}^{\mathrm{NS}}_{k,(\varphi,m)}(\tau,\nu) \approx \left|\frac{\vartheta_3(\tau,\nu)}{\eta^3(\tau)}\right|^2 \mathrm{e}^{\mathrm{i}m\varphi}\frac{\sqrt{k+2}}{2}\int \mathrm{d}p\,(q\bar{q})^{p^2/4}, \tag{3.8}$$

where we employed the Euler–MacLaurin sum formula (see, e.g., [13, appendix D]) to convert the sum over l into an integral over $p = l/\sqrt{k+2}$. For fixed m and large l all singular vectors disappear and $\Gamma^{(k)}_{lm} \to 1$. To get the true partition function, i.e. the trace over the projected Hilbert space, we have to combine $\mathcal{P}$ evaluated at ν and at $\nu + \mathrm{i}\pi$, and we find after rescaling by an overall factor

$$\frac{1}{\sqrt{k+2}}\left(\mathcal{P}^{\mathrm{NS}}_{k,(\varphi)}(\tau,\nu) + \mathcal{P}^{\mathrm{NS}}_{k,(\varphi)}(\tau,\nu+\mathrm{i}\pi)\right)$$

$$\to \frac{1}{2}\left(\left|\frac{\vartheta_3(\tau,\nu)}{\eta^3(\tau)}\right|^2 + \left|\frac{\vartheta_4(\tau,\nu)}{\eta^3(\tau)}\right|^2\right)\sum_{m\in\mathbb{Z}}\mathrm{e}^{\mathrm{i}m\varphi}\int_0^\infty \mathrm{d}p(q\bar{q})^{p^2/4}, \tag{3.9}$$

---

[1] Consider, e.g., a free compact bosonic field $\phi \equiv \phi + 2\pi R$. For $R \to \infty$ the partition function diverges as the volume R, and for the noncompact boson one usually considers the regularized partition function rescaled by $1/R$.

which is precisely the Neveu–Schwarz part of the partition function of two free uncompactified bosons and two fermions (see, e.g., [14, chapter 12.2]), weighted by the rotation operator $e^{iM\varphi}$. The rescaling can be explained from the analysis in the following subsection: in the interval $[p, p + \Delta p]$ there are $\frac{\sqrt{k+2}}{2}\Delta p$ ground states contributing to the partition function (see (3.12)). The rescaling therefore corresponds to adjusting the density of states to 1 per unit interval Δp.

3.2. Fields and correlators

We will now define fields $\Phi_{p,m}$ in the limit theory, which arise from averaged fields $^{(2)}\Phi_f^{(k)}$ with specific averaging functions f. For $m = 0$, the behaviour of the corresponding fields in the limit was analysed in [8], and we will closely follow that construction.

In the Neveu–Schwarz sector of the kth minimal model we introduce the averaged fields[2]

$$\Phi_{p,m}^{\epsilon,k} = \frac{1}{|N(p, \epsilon, k, m)|} \sum_{l \in N(p,\epsilon,k,m)} \phi_{l,m}, \tag{3.10}$$

where $\phi_{l,m}$ are Neveu–Schwarz primary fields (labelled by two integers with $0 \leqslant l \leqslant k$, $|m| \leqslant l$ and $l + m$ even), and the set $N(p, \epsilon, k, m)$ contains all allowed labels l that are close to $p\sqrt{k+2}$,

$$N(p, \epsilon, k, m) = \left\{ l : l + m \text{ even}, \ p - \frac{\epsilon}{2} < \frac{l}{\sqrt{k+2}} < p + \frac{\epsilon}{2} \right\}. \tag{3.11}$$

Here, ϵ is a small real number that will be taken to zero at the end. For large k the number of elements in $N(p, \epsilon, k, m)$ is (assuming $p - \frac{\epsilon}{2} > 0$)

$$|N(p, \epsilon, k, m)| = \epsilon \frac{\sqrt{k+2}}{2} + \mathcal{O}(1). \tag{3.12}$$

These averaged fields are used to define fields $\Phi_{p,m}$ in the limit theory of conformal weight $h = \frac{p^2}{4}$ and $U(1)$ charge $Q = 0$. Their correlators are defined as

$$\langle \Phi_{p_1,m_1}(z_1, \bar{z}_1) \cdots \Phi_{p_r,m_r}(z_r, \bar{z}_r) \rangle$$
$$= \lim_{\epsilon \to 0} \lim_{k \to \infty} \beta(k)^2 \alpha(k)^r \langle \Phi_{p_1,m_1}^{\epsilon,k}(z_1, \bar{z}_1) \cdots \Phi_{p_r,m_r}^{\epsilon,k}(z_r, \bar{z}_r) \rangle, \tag{3.13}$$

with normalization factors $\alpha(k)$ for each field, and an overall normalization factor $\beta^2(k)$ for correlators on the sphere. In addition to this rescaling we also have the possibility to redefine the fields $\phi_{l,m}$ by individual phases. Compared to the analysis in [8] we change the normalization by

$$\phi_{l,m} \to (-1)^{\frac{l-m}{2}} \phi_{l,m}. \tag{3.14}$$

The necessity of introducing these signs will become clear when we analyse the three-point function. With this convention the two-point function in the minimal models is

$$\langle \phi_{l_1,m_1}(z_1, \bar{z}_1) \phi_{l_2,m_2}(z_2, \bar{z}_2) \rangle = (-1)^{\frac{l_1-m_1+l_2-m_2}{2}} \delta_{l_1,l_2} \delta_{m_1+m_2,0} \frac{1}{|z_{12}|^{4h_1}}$$
$$= (-1)^{m_1} \delta_{l_1,l_2} \delta_{m_1+m_2,0} \frac{1}{|z_{12}|^{4h_1}}, \tag{3.15}$$

where we used that $l_1 + m_1$ is even.

---

[2] In comparison to the discussion around (1.3) we make use of the fact that the spectrum of the rescaled charge $Q(k+2) = -m$ is discrete so that we can define fields with fixed labels m. For large k our procedure here then corresponds to using a (discontinuous) averaging function $f_{p,\epsilon}(h) = \begin{cases} 1/\epsilon & \text{for } |p - 2\sqrt{h}| < \epsilon/2 \\ 0 & \text{else} \end{cases}$, and in addition a k-dependent rescaling of the fields by $2/\sqrt{k+2}$.

By following the analysis of [8] we find a normalized two-point function in the limit,

$$\langle \Phi_{p_1,m_1}(z_1,\bar{z}_1)\Phi_{p_2,m_2}(z_2,\bar{z}_2)\rangle = (-1)^{m_1}\delta(p_1-p_2)\delta_{m_1+m_2,0}\frac{1}{|z_1-z_2|^{p_1^2}}, \tag{3.16}$$

if we choose

$$\alpha(k)\beta(k) = \frac{(k+2)^{1/4}}{\sqrt{2}}. \tag{3.17}$$

Before moving on, let us compare this to the free field theory of two uncompactified bosons and two fermions. The primary fields $\Phi_{\mathbf{p}}^{\text{free}}$ in the Neveu–Schwarz sector are labelled by a complex momentum $\mathbf{p}$, they have conformal weight $h = \frac{|\mathbf{p}|^2}{4}$ and $U(1)$ charge $q = 0$. We can define a new 'radial' basis,

$$\Phi_{p,m}^{\text{free}} = \sqrt{\frac{p}{2\pi}}\int \mathrm{d}\varphi\, \Phi_{p e^{i\varphi}}^{\text{free}}\, e^{im\varphi}, \tag{3.18}$$

where the factor in front ensures a proper normalization of the two-point function,

$$\langle \Phi_{p_1,m_1}^{\text{free}}(z_1,\bar{z}_1)\Phi_{p_2,m_2}^{\text{free}}(z_2,\bar{z}_2)\rangle = (-1)^{m_1}\delta(p_1-p_2)\delta_{m_1+m_2,0}\frac{1}{|z_1-z_2|^{p_1^2}}. \tag{3.19}$$

We therefore expect that the fields $\Phi_{p,m}$ of the limit theory are to be identified with the fields $\Phi_{p,m}^{\text{free}}$ of the free field theory. To confirm this we now look at the three-point function.

3.3. Three-point function

The three-point function in the free theory is given by

$$\langle \Phi_{\mathbf{p}_1}^{\text{free}}(z_1,\bar{z}_1)\Phi_{\mathbf{p}_2}^{\text{free}}(z_2,\bar{z}_2)\Phi_{\mathbf{p}_3}^{\text{free}}(z_3,\bar{z}_3)\rangle = \delta^{(2)}(\mathbf{p}_1+\mathbf{p}_2+\mathbf{p}_3)$$
$$\times |z_{12}|^{2(h_3-h_1-h_2)}|z_{23}|^{2(h_1-h_2-h_3)}|z_{13}|^{2(h_2-h_1-h_3)}. \tag{3.20}$$

A straightforward calculation (see appendix C) shows that in the basis $\Phi_{p,m}^{\text{free}}$ it can be expressed as

$$\langle \Phi_{p_1,m_1}^{\text{free}}(z_1,\bar{z}_1)\Phi_{p_2,m_2}^{\text{free}}(z_2,\bar{z}_2)\Phi_{p_3,m_3}^{\text{free}}(z_3,\bar{z}_3)\rangle = \delta_{m_1+m_2+m_3,0}\frac{\sqrt{p_1 p_2 p_3}}{\sqrt{2\pi}}(-1)^{m_3}$$
$$\times \frac{\cos(m_2\alpha_1-m_1\alpha_2)}{A(p_1,p_2,p_3)}|z_{12}|^{2(h_3-h_1-h_2)}|z_{23}|^{2(h_1-h_2-h_3)}|z_{13}|^{2(h_2-h_1-h_3)}, \tag{3.21}$$

where $A(p_1,p_2,p_3)$ is the area of the triangle with side lengths p_1, p_2 and p_3, and α_i is the angle of the triangle opposite of the edge p_i. If a triangle with these side lengths does not exist, the correlator is zero.

The three-point functions in the limit theory are obtained from the three-point functions in the minimal models [15] (see also [16, 17]). For large $k+2$ and $l_i \approx p_i\sqrt{k+2}$, the three-point function is given by (see [8])

$$\langle \phi_{l_1,m_1}(z_1,\bar{z}_1)\phi_{l_2,m_2}(z_2,\bar{z}_2)\phi_{l_3,m_3}(z_3,\bar{z}_3)\rangle = (-1)^{\frac{l_1+l_2+l_3}{2}}\begin{pmatrix} \frac{l_1}{2} & \frac{l_2}{2} & \frac{l_3}{2} \\ \frac{m_1}{2} & \frac{m_2}{2} & \frac{m_3}{2} \end{pmatrix}^2$$
$$\times \sqrt{(l_1+1)(l_2+1)(l_3+1)}\,\delta_{m_1+m_2+m_3,0}|z_{12}|^{2(h_3-h_1-h_2)}|z_{13}|^{2(h_2-h_1-h_3)}|z_{23}|^{2(h_1-h_2-h_3)}. \tag{3.22}$$

Here, $\begin{pmatrix} j_1 & j_2 & j_3 \\ \mu_1 & \mu_2 & \mu_3 \end{pmatrix}$ denotes the Wigner $3j$-symbols, and in order to determine the correlator in the limit one has to understand the asymptotic behaviour of the $3j$-symbols for large quantum numbers j_i, which we analyse in appendix B. The result (compare with (B.14)) is

$$\begin{pmatrix} \frac{l_1}{2} & \frac{l_2}{2} & \frac{l_3}{2} \\ \frac{m_1}{2} & \frac{m_2}{2} & \frac{m_3}{2} \end{pmatrix} = (k+2)^{-1/2}\frac{(-1)^{\frac{l_1-l_2-m_3}{2}}}{\sqrt{\frac{\pi}{2}A(p_1,p_2,p_3)}}$$
$$\times \cos\left(\frac{l_1+l_2-l_3}{4}\pi + \frac{m_2\alpha_1-m_1\alpha_2}{2}\right) + \mathcal{O}(k^{-1}). \tag{3.23}$$

8

For large level k the three-point function therefore behaves as

$$\langle \phi_{l_1,m_1}(z_1,\bar{z}_1)\phi_{l_2,m_2}(z_2,\bar{z}_2)\phi_{l_3,m_3}(z_3,\bar{z}_3)\rangle = (k+2)^{-1/4}\frac{2\sqrt{p_1p_2p_3}}{\pi A(p_1,p_2,p_3)}\delta_{m_1+m_2+m_3,0}$$
$$\times (-1)^{\frac{l_1+l_2+l_3}{2}}\cos^2\left(\frac{l_1+l_2-l_3}{4}\pi + \frac{m_2\alpha_1-m_1\alpha_2}{2}\right)$$
$$\times |z_{12}|^{2(h_3-h_1-h_2)}|z_{13}|^{2(h_2-h_1-h_3)}|z_{23}|^{2(h_1-h_2-h_3)}. \tag{3.24}$$

To obtain the correlator in the limit theory we have to average over the quantum numbers l_i. We observe that

$$(-1)^{\frac{l_1+l_2+l_3}{2}}\cos^2\left(\frac{l_1+l_2-l_3}{4}\pi + \frac{m_2\alpha_1-m_1\alpha_2}{2}\right)$$
$$= (-1)^{m_3}\times\begin{cases}\cos^2\left(\frac{m_2\alpha_1-m_1\alpha_2}{2}\right) & \text{for } \frac{l_1+l_2-l_3}{2}=0 \text{ mod } 2 \\ -\sin^2\left(\frac{m_2\alpha_1-m_1\alpha_2}{2}\right) & \text{for } \frac{l_1+l_2-l_3}{2}=1 \text{ mod } 2.\end{cases} \tag{3.25}$$

In average these contributions combine to

$$\frac{1}{2}(-1)^{m_3}\left(\cos^2\frac{m_2\alpha_1-m_1\alpha_2}{2} - \sin^2\frac{m_2\alpha_1-m_1\alpha_2}{2}\right) = \frac{1}{2}(-1)^{m_3}\cos(m_2\alpha_1-m_1\alpha_2). \tag{3.26}$$

In total we arrive at

$$\langle \Phi_{p_1,m_1}(z_1,\bar{z}_1)\Phi_{p_2,m_2}(z_2,\bar{z}_2)\Phi_{p_3,m_3}(z_3,\bar{z}_3)\rangle = \beta^2(k)\alpha^3(k)(k+2)^{-1/4}\delta_{m_1+m_2+m_3,0}(-1)^{m_3}$$
$$\times \frac{\sqrt{p_1p_2p_3}}{\pi}\frac{\cos(m_2\alpha_1-m_1\alpha_2)}{A(p_1,p_2,p_3)}|z_{12}|^{2(h_3-h_1-h_2)}|z_{23}|^{2(h_1-h_2-h_3)}|z_{13}|^{2(h_2-h_1-h_3)}, \tag{3.27}$$

which matches the free field theory result (3.21) if we set (respecting (3.17))

$$\alpha(k) = \sqrt{2\pi}(k+2)^{-1/4}, \qquad \beta(k) = \frac{1}{2\sqrt{\pi}}(k+2)^{1/2}. \tag{3.28}$$

Hence, we find perfect agreement for the three-point function. Notice that the redefinition of the minimal model fields $\phi_{l,m}$ by the sign $(-1)^{\frac{l-m}{2}}$ was crucial in matching the expressions. Without it, the averaging in (3.26) would simply give $\frac{1}{2}(-1)^{m_3}$ so that the three-point function would have a rather trivial dependence on the labels m_i.

3.4. A-type boundary conditions

We now want to discuss boundary conditions. In a free theory the simplest boundary conditions we can discuss are combinations of Dirichlet and Neumann boundary conditions, and interpreting the free bosonic fields as coordinates of a flat target space, such boundary conditions can be formulated by specifying a flat submanifold (brane) that encodes the possible boundary values of the fields. We first focus on one-dimensional branes in our two-dimensional target. By choosing boundary conditions also for the fermions, we can ensure appropriate boundary conditions for the supercurrents such that the maximal amount of supersymmetry is preserved. For our one-dimensional branes, this leads to A-type gluing conditions for the supercurrents (for a discussion of A- and B-type gluing conditions in $N=2$ supersymmetric field theories see e.g. [18, 19]). In the free theory, a one-dimensional brane is characterized
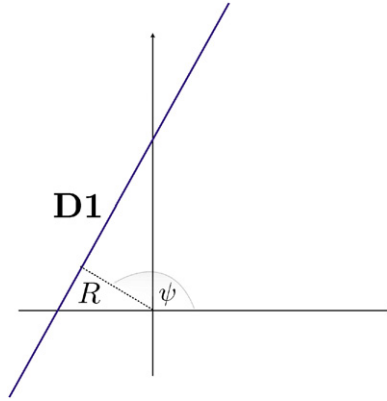
Figure 1. Illustration of the boundary condition that corresponds to a one-dimensional brane, and the distance R and the angle ψ that determine its position.

by a vector $Re^{i\psi}$ that determines its shortest distance from the origin plus an orientation (see figure 1). In the Neveu–Schwarz sector the one-point functions are[3]

$$\left\langle \Phi^{\text{free}}_{pe^{i\varphi}}(z,\bar{z}) \right\rangle^{A}_{R,\psi} = \frac{1}{2} \delta(p \cos(\psi - \varphi)) \, e^{iRp\sin(\psi-\varphi)} \frac{1}{|z - \bar{z}|^{2h_p}}. \tag{3.29}$$

The prefactor $1/2$ already includes the factor of $2^{-1/2}$ that arises because we choose the (GSO-like) projection of our theory such that also the Ramond–Ramond fields couple to the one-dimensional brane. In the radial basis, the one-point function is then given by

$$\left\langle \Phi^{\text{free}}_{p,m}(z,\bar{z}) \right\rangle^{A}_{R,\psi} = \sqrt{\frac{p}{2\pi}} \int d\varphi \, e^{im\varphi} \left\langle \Phi^{\text{free}}_{pe^{i\varphi}}(z,\bar{z}) \right\rangle^{A}_{R,\psi} \tag{3.30}$$

$$= \frac{1}{\sqrt{2\pi p}} e^{im\psi} \cdot \begin{cases} \cos Rp & \text{for } m \text{ even} \\ i\sin Rp & \text{for } m \text{ odd.} \end{cases} \tag{3.31}$$

In the minimal models, A-type boundary conditions are obtained using the standard Cardy construction [20]. They are labelled by integers (L, M, S), where $0 \leqslant L \leqslant k$, M is $2k + 4$-periodic, $S \in \{-1, 0, 1, 2\}$, and $L + M + S$ is even. In the geometric description (2.1) of [12], these boundary conditions correspond to branes that are straight lines characterized by the equation

$$\rho \cos(\varphi - \varphi_0) = \rho_0, \tag{3.32}$$

where

$$\rho_0 = \cos\frac{\pi(L+1)}{k+2}, \quad \varphi_0 = \frac{\pi M}{k+2}. \tag{3.33}$$

---

[3] A boundary condition corresponding to a d-dimensional brane in a D-dimensional target space that only couples to the NS–NS sector has the one-point function

$$\left\langle e^{i\vec{p}\cdot\vec{X}} \right\rangle = 2^{-\frac{D}{4}}(\alpha')^{\frac{D-2d}{4}} \delta^{(d)}(\vec{p}_\parallel) e^{i\vec{R}\cdot\vec{p}_\perp} |z - \bar{z}|^{-2h_p},$$

where the conformal weight is $h_p = \frac{\alpha' p^2}{4}$. The projection of the full Hilbert space only allows either the even- or the odd-dimensional branes to couple to the R–R sector; in that case there is an additional factor of $2^{-1/2}$. In our conventions $\alpha' = 1$.

Note that boundary labels (L, M, S) and $(k - L, M + k + 2, S + 2)$ describe the same boundary conditions, and we can always choose $L \leqslant k/2$ such that the above defined ρ_0 is positive. In the geometric picture (ρ_0, φ_0) are the coordinates of the point on the brane that is closest to the origin. For large k the distance to the origin is given by $\rho_0' = \sqrt{k+2}\,\rho_0$. To make contact with the free field theory description we want this distance to approach the constant R,

$$\sqrt{k+2} \cos \frac{\pi(L+1)}{k+2} \to R. \tag{3.34}$$

We can achieve this by scaling the boundary label as

$$L = \frac{1}{2}(k+2) - \frac{R}{\pi}\sqrt{k+2} + \mathcal{O}(1). \tag{3.35}$$

Similarly we scale the boundary label M such that the corresponding angle φ_0 is constant in the limit,

$$M = \frac{k+2}{\pi}\varphi_0 + \mathcal{O}(1). \tag{3.36}$$

We expect φ_0 to coincide with the angle ψ up to a possible additive shift.

The one-point function of a Neveu–Schwarz primary field $\phi_{l,m}$ for a boundary condition (L, M, S) is given by (see[4], e.g., [12])

$$\langle \phi_{l,m}(z, \bar{z}) \rangle^A_{(L,M,S)} = \frac{(-1)^{\frac{l-m}{2}}}{\sqrt{k+2}} \frac{\sin \frac{\pi(l+1)(L+1)}{k+2}}{\sqrt{\sin \frac{\pi(l+1)}{k+2}}} e^{\pi i \frac{Mm}{k+2}} \frac{1}{|z - \bar{z}|^{2h_{l,m}}}. \tag{3.37}$$

For L and M as in (3.35) and (3.36), this behaves as

$$\langle \phi_{l,m}(z, \bar{z}) \rangle^A_{(L,M,S)} = \frac{(k+2)^{-1/4}}{2\sqrt{\pi p}} \left(e^{iR\frac{l+1}{\sqrt{k+2}}} - e^{i\pi(l+1) - iR\frac{l+1}{\sqrt{k+2}}} \right) e^{i(\varphi_0 - \frac{\pi}{2})m} \frac{1}{|z - \bar{z}|^{2h_{l,m}}}. \tag{3.38}$$

To obtain the one-point function for the limit field $\Phi_{p,m}$ we take expression (3.38), multiply it by $\alpha(k)\beta(k)$ given in (3.17) and take the limit $k \to \infty$ while we keep m constant and scale $l \approx p\sqrt{k+2}$. We arrive at the result

$$\langle \Phi_{p,m} \rangle^A_{R,\varphi_0} = \frac{1}{\sqrt{2\pi p}} e^{i(\varphi_0 - \frac{\pi}{2})m} \cdot \begin{cases} \cos Rp & \text{for } m \text{ even} \\ i \sin Rp & \text{for } m \text{ odd}, \end{cases} \tag{3.39}$$

which precisely matches the free field theory result (3.31) upon identifying $\psi = \varphi_0 - \frac{\pi}{2}$.

3.5. B-type boundary conditions

B-type boundary conditions in minimal models are labelled by two integers (L, S) where $0 \leqslant L \leqslant k$ and $S = 0, 1$. The one-point functions of Neveu–Schwarz primaries are given by (see[5] e.g. [12])

$$\langle \phi_{l,m}(z, \bar{z}) \rangle^B_{(L,S)} = \sqrt{2} \frac{\sin \frac{\pi(l+1)(L+1)}{k+2}}{\sqrt{\sin \frac{\pi(l+1)}{k+2}}} \delta_{m,0} |z - \bar{z}|^{-2h_{l,m}}. \tag{3.40}$$

Geometrically these correspond to two-dimensional discs [12] where the coordinate of the boundary is given by $\rho_1 = \sin \frac{\pi(L+1)}{k+2}$. We expect that we can define two limits: one for which the disc shrinks to a point to describe a zero-dimensional brane in the free theory, and one for which the disc covers the whole plane corresponding to a two-dimensional brane in the free theory.

---

[4] The sign $(-1)^{\frac{l-m}{2}}$ comes from our field redefinition in (3.14).
[5] Note that the sign $(-1)^{\frac{l-m}{2}}$ that one expects from the field redefinition (3.14) is absorbed by a sign hidden inside the definition of the B-type Ishibashi states in [12].

Let us first consider the zero-dimensional brane. We keep the label L fixed, such that the radius of the disc, $\rho'_1 = \sqrt{k+2} \sin \frac{\pi(L+1)}{k+2}$, goes to zero. One readily obtains the corresponding one-point function

$$\left\langle \Phi_{p,m}(z, \bar{z}) \right\rangle^B_{(L,S)} = \sqrt{\pi p}(L+1)\delta_{m,0}|z - \bar{z}|^{-2h_p}, \tag{3.41}$$

which is an integer multiple of the one-point function for $L = 0$, so it describes a stack of $L+1$ elementary branes. This is related to the fact that in minimal models the B-type boundary conditions with $L > 0$ can be obtained from a superposition of boundary conditions with $L = 0$ by a boundary renormalization group flow that becomes short when $k \to \infty$ [21].

In the free theory, for a zero-dimensional brane at the origin, the one-point function of Neveu–Schwarz primary fields Φ_p^{free} is simply[6]

$$\left\langle \Phi_{\mathbf{p}}^{\text{free}}(z, \bar{z}) \right\rangle^B_{(0)} = \frac{1}{\sqrt{2}}|z - \bar{z}|^{-2h_p}, \tag{3.42}$$

which in the radial basis reads

$$\left\langle \Phi_{p,m}^{\text{free}}(z, \bar{z}) \right\rangle^B_{(0)} = \sqrt{\pi p}\,\delta_{m,0} \frac{1}{|z - \bar{z}|^{2h_p}}, \tag{3.43}$$

in precise agreement with the minimal model computation.

On the other hand, we can look at two-dimensional branes. There is a one-parameter family of those that differ in the strength of a constant electric background field. The electric field can be labelled by an angle[7] $-\pi < \phi < \pi$ (see e.g. [22, 23] and the discussion in [24]). The boundary conditions are characterized by the one-point functions

$$\left\langle \Phi_{\mathbf{p}}^{\text{free}}(z, \bar{z}) \right\rangle^B_{\phi} = \frac{1}{\sqrt{2}\cos\frac{\phi}{2}}\delta^{(2)}(\mathbf{p}). \tag{3.44}$$

Instead of working with the delta distribution directly, it is more convenient to apply it on a test function $\zeta(\mathbf{p})$, i.e. we look at a smeared one-point function

$$\left\langle \int d^2 p\, \zeta(\mathbf{p}) \Phi_{\mathbf{p}}^{\text{free}}(z, \bar{z}) \right\rangle^B_{\phi} = \frac{1}{\sqrt{2}\cos\frac{\phi}{2}}\zeta(0). \tag{3.45}$$

For a comparison to the minimal model limit, we express it in terms of the radial basis,

$$\left\langle \int dp \sum_m \zeta_{p,-m} \Phi_{p,m}^{\text{free}}(z, \bar{z}) \right\rangle^B_{\phi} = \left\langle \int d^2 p\, \zeta(\mathbf{p}) \Phi_{\mathbf{p}}^{\text{free}}(z, \bar{z}) \right\rangle^B_{\phi} = \frac{1}{\sqrt{2}\cos\frac{\phi}{2}}\zeta(0) \tag{3.46}$$

$$= \frac{1}{\sqrt{2}\cos\frac{\phi}{2}}\frac{\zeta_{p,0}}{\sqrt{2\pi p}}\bigg|_{p=0}, \tag{3.47}$$

where

$$\zeta_{p,m} = \sqrt{\frac{p}{2\pi}}\int d\varphi\, e^{im\varphi}\zeta(pe^{i\varphi}). \tag{3.48}$$

We can reformulate this as

$$\left\langle \Phi_{p,m}^{\text{free}}(z, \bar{z}) \right\rangle^B_{\phi} = 0 \qquad \text{for } m \neq 0 \tag{3.49a}$$

$$\left\langle \sqrt{2\pi} \int_0^\infty dp \sqrt{p}\chi(p) \Phi_{p,0}^{\text{free}}(z, \bar{z}) \right\rangle^B_{\phi} = \frac{1}{\sqrt{2}\cos\frac{\phi}{2}}\chi(0), \tag{3.49b}$$

for suitable test functions χ on the positive real line.

---

[6] Note that the zero-dimensional brane cannot couple to the R-R sector, because we chose the projection such that the one-dimensional brane couples to it. Therefore the prefactor is simply $2^{-D/4} = 2^{-1/2}$ (compare the discussion in footnote 3 on page 10).

[7] Where $\sin\phi = \frac{2f}{1+f^2}$ and $\cos\phi = \frac{1-f^2}{1+f^2}$ for an electric field strength $F_{\mu\nu} = \begin{pmatrix} 0 & f \\ -f & 0 \end{pmatrix}$.

We expect to get these boundary conditions from the minimal models by considering B-type boundary conditions that correspond to a disc covering the whole two-dimensional space in the minimal model geometry. These are labelled by (L, S) where L is scaled linearly with k, $L = \lfloor \Lambda(k+2) \rfloor$. The minimal model one-point functions behave as

$$\langle \phi_{l,m}(z, \bar{z}) \rangle^B_{(\lfloor \Lambda(k+2) \rfloor, S)} \approx \sqrt{\frac{2(k+2)}{\pi(l+1)}} \, \sin\left(\pi \Lambda(l+1)\right) \delta_{m,0} |z - \bar{z}|^{-2h_{l,m}}. \quad (3.50)$$

The sine function in the numerator oscillates rapidly as a function of l. Therefore the one-point function of $\Phi_{p,0}$ is suppressed for non-zero p as expected. To evaluate the contribution at $p = 0$, we consider the one-point function for fields smeared by a test function χ,

$$
\begin{aligned}
&\left\langle \sqrt{2\pi} \int_0^\infty \mathrm{d}p \, \sqrt{p} \chi(p) \Phi_{p,0}(z, \bar{z}) \right\rangle^B_{(\lfloor \Lambda(k+2) \rfloor, S)} \\
&= \lim_{k \to \infty} \sqrt{2\pi} \sqrt{2} (k+2)^{-1/4} \sum_{l \text{ even}} \left(\frac{l+1}{\sqrt{k+2}}\right)^{\frac{1}{2}} \chi\left(\frac{l+1}{\sqrt{k+2}}\right) \langle \phi_{l,0}(z, \bar{z}) \rangle^B_{(\lfloor \Lambda(k+2) \rfloor, S)} \\
&= \lim_{k \to \infty} 2\sqrt{2} \sum_{l \text{ even}} \sin\left(\pi \Lambda(l+1)\right) \chi\left(\frac{l+1}{\sqrt{k+2}}\right) |z - \bar{z}|^{-2h_{l,0}} \\
&= \frac{\sqrt{2}}{\sin \pi \Lambda} \chi(0), \quad\quad\quad\quad\quad\quad\quad\quad\quad\quad\quad\quad\quad\quad\quad\quad\quad\quad\quad\quad (3.51)
\end{aligned}
$$

which equals twice the result in equation (3.49b) if we set

$$\phi = \pm 2\pi \left(\Lambda - \frac{1}{2}\right). \quad (3.52)$$

Therefore the limiting boundary condition is not elementary, but a superposition of two two-dimensional branes in the free theory. A closer analysis (e.g. by looking at the relative spectrum to the zero-dimensional brane) reveals that in fact it is a superposition of two branes with opposite electric field (corresponding to the two possible signs of ϕ in (3.52)). This is in accordance with the identification of B-type boundary states in minimal models under $L \leftrightarrow k - L$, which amounts to the identification $\Lambda \leftrightarrow 1 - \Lambda$ corresponding to a switch of the sign in (3.52).

This concludes our discussion of the free field limit, and we turn now to the continuous orbifold limit.

4. Continuous orbifold limit

In [8] we constructed a limit of minimal models where both field labels l and m are sent to infinity such that both the conformal weight and the $U(1)$ charge are kept fixed. The resulting theory contains a spectrum of primary fields that is continuous in the $U(1)$ charge. In this section we want to interpret this limit as a continuous orbifold of a free theory, where the $U(1)$ charge serves as a twist parameter.

The possibility to construct continuous orbifolds by gauging a continuous global symmetry group was recently explored in [25] where the non-Abelian orbifold $SU(2)_1/SO(3)$ was analysed. The theory we want to consider is the $N = (2, 2)$ supersymmetric theory of two uncompactified bosons and two fermions orbifolded by the rotation group $SO(2) \simeq U(1)$.

4.1. The orbifold

Notations and conventions follow closely the ones in [24]. We start by defining the real bosonic coordinates $X^1(z, \bar{z}), X^2(z, \bar{z})$ and their fermionic counterparts $\psi^1(z, \bar{z}), \psi^2(z, \bar{z})$.

We rearrange the fields to work on the complex plane with one free complex fermion, namely defining

$$\phi = \frac{1}{\sqrt{2}}(X^1 + iX^2), \quad \phi^* = \frac{1}{\sqrt{2}}(X^1 - iX^2), \tag{4.1a}$$

$$\psi = \frac{1}{\sqrt{2}}(\psi^1 + i\psi^2) \quad \psi^* = \frac{1}{\sqrt{2}}(\psi^1 - i\psi^2), \tag{4.1b}$$

such that the mode expansion of the (holomorphic) fields reads

$$\partial\phi = -i\sum_{m\in\mathbb{Z}} \alpha_m z^{-m-1}, \quad \partial\phi^* = -i\sum_{m\in\mathbb{Z}} \alpha_m^* z^{-m-1}, \tag{4.2a}$$

$$\psi = \sum_{r\in\mathbb{Z}+\eta} \psi_r z^{-r-\frac{1}{2}}, \quad \psi^* = \sum_{r\in\mathbb{Z}+\eta} \psi_r^* z^{-r-\frac{1}{2}}, \tag{4.2b}$$

where $\eta = 0, \frac{1}{2}$ in the Ramond and Neveu–Schwarz sector, respectively. The antiholomorphic case is analogous. For simplicity we will restrict the following discussion to the Neveu–Schwarz sector. The modes respect the algebra of one free complex boson and one free Neveu–Schwarz complex fermion:

$$[\alpha_m, \alpha_n^*] = m\delta_{m,-n}, \quad \{\psi_r, \psi_s^*\} = \delta_{r,-s}, \tag{4.3a}$$

$$[\alpha_m, \alpha_n] = [\alpha_m^*, \alpha_n^*] = 0, \quad \{\psi_r, \psi_s\} = \{\psi_r^*, \psi_s^*\} = 0. \tag{4.3b}$$

We can explicitly realize the $N = 2$ superconformal algebra by defining the generators through our holomorphic fields as

$$T = -\partial\phi\partial\phi^* - \frac{1}{2}(\psi^*\partial\psi + \psi\partial\psi^*), \quad J = -\psi^*\psi, \tag{4.4a}$$

$$G^+ = i\sqrt{2}\psi\partial\phi^*, \quad G^- = i\sqrt{2}\psi^*\partial\phi, \tag{4.4b}$$

and similarly for their antiholomorphic counterparts.

We want to end up with an $N = (2, 2)$ theory; we therefore choose the action of the orbifold group in such a way that the currents in (4.4) are invariant under the transformation and supersymmetry is not broken. In particular we choose the $U(1)$ action on the fields as follows

$$U(\theta) \cdot \phi = e^{i\theta}\phi, \quad U(\theta) \cdot \phi^* = e^{-i\theta}\phi^*, \tag{4.5a}$$

$$U(\theta) \cdot \psi = e^{i\theta}\psi, \quad U(\theta) \cdot \psi^* = e^{-i\theta}\psi^*, \tag{4.5b}$$

so that in terms of the coordinates X^1, X^2 on the plane it is realized by the rotation matrix

$$U(\theta) \cdot \vec{X} \equiv \mathcal{R}_\theta \cdot \vec{X} = \begin{pmatrix} \cos\theta & -\sin\theta \\ \sin\theta & \cos\theta \end{pmatrix} \cdot \begin{pmatrix} X^1 \\ X^2 \end{pmatrix}. \tag{4.6}$$

The action of the group on the field modes is thus

$$\alpha_n \mapsto e^{i\theta}\alpha_n, \quad \alpha_n^* \mapsto e^{-i\theta}\alpha_n^*, \tag{4.7a}$$

$$\psi_r \mapsto e^{i\theta}\psi_r, \quad \psi_r^* \mapsto e^{-i\theta}\psi_r^*. \tag{4.7b}$$

4.2. Partition function

We now want to determine the partition function of the orbifold. We first look at the Neveu–Schwarz part, and work with the full supersymmetric Hilbert space. To compare with the minimal models we will later perform a (GSO-like) projection by $\frac{1}{2}(1 + (-1)^{F+\bar{F}})$ onto states of even fermion number.

By inserting a twist operator we obtain the θ-twined characters

$$\theta \;\square_0 = \mathrm{Tr}_{\mathcal{H}_{\mathrm{free}}^{\mathrm{NS}}} \left(U(\theta) q^{L_0 - \frac{1}{8}} \bar{q}^{\bar{L}_0 - \frac{1}{8}} \right), \tag{4.8}$$

where we denoted by $\mathcal{H}_{\mathrm{free}}^{\mathrm{NS}}$ the (unprojected) Neveu–Schwarz part of the Hilbert space of the free theory.

The orbifold group acts non-trivially on the vacua labelled by the momentum on the plane,

$$|\vec{p}\rangle \longmapsto |\mathcal{R}_\theta \cdot \vec{p}\rangle, \tag{4.9}$$

so that the momentum dependent part of equation (4.8) becomes

$$\int \mathrm{d}^2 p \, \delta^2(\mathcal{R}_\theta \cdot \vec{p} - \vec{p}) \, (q\bar{q})^{\frac{|\vec{p}|^2}{4}} = \int \mathrm{d}^2 p \, \frac{1}{\det(\mathcal{R}_\theta - 1)} \delta^2(\vec{p}) \, (q\bar{q})^{\frac{|\vec{p}|^2}{4}}. \tag{4.10}$$

The θ-twined character is then

$$\theta \;\square_0 = \mathrm{Tr}_{\mathcal{H}_{\mathrm{free}}^{\mathrm{NS}}} \left(U(\theta) q^{L_0 - \frac{1}{8}} \bar{q}^{\bar{L}_0 - \frac{1}{8}} \right)$$

$$= \int \mathrm{d}^2 p \, \frac{\delta^2(\vec{p})}{\det(\mathcal{R}_\theta - 1)} \, (q\bar{q})^{\frac{|\vec{p}|^2}{4}} \left| q^{-\frac{1}{8}} \prod_{n=0}^{\infty} \frac{(1 + q^{n+\frac{1}{2}} \mathrm{e}^{\mathrm{i}\theta})(1 + q^{n+\frac{1}{2}} \mathrm{e}^{-\mathrm{i}\theta})}{(1 - q^{n+1} \mathrm{e}^{\mathrm{i}\theta})(1 - q^{n+1} \mathrm{e}^{-\mathrm{i}\theta})} \right|^2$$

$$= \left| \frac{\vartheta_3(\tau, \frac{\theta}{2\pi})}{\vartheta_1(\tau, \frac{\theta}{2\pi})} \right|^2. \tag{4.11}$$

We then act with a modular S-transformation on the complex modulus of the torus ($\tau \mapsto -\frac{1}{\tau}$) to get from the θ-twined free character to the character of the θ-twisted sector,

$$\theta \;\square_0 \quad \overset{S}{\longmapsto} \quad 0 \;\square_\theta. \tag{4.12}$$

We can benefit from known transformation properties of the ϑ-functions, in particular

$$\frac{\vartheta_3(-\frac{1}{\tau}, \nu)}{\vartheta_1(-\frac{1}{\tau}, \nu)} = i \frac{\vartheta_3(\tau, \nu\tau)}{\vartheta_1(\tau, \nu\tau)}, \tag{4.13}$$

so that the θ-twisted sector reads

$$0 \;\square_\theta = \mathrm{Tr}_{\mathcal{H}_\theta^{\mathrm{NS}}} \left(q^{L_0 - \frac{1}{8}} \bar{q}^{\bar{L}_0 - \frac{1}{8}} \right) = \left| \frac{\vartheta_3(\tau, \frac{\tau\theta}{2\pi})}{\vartheta_1(\tau, \frac{\tau\theta}{2\pi})} \right|^2, \tag{4.14}$$

$$= \left| q^{-\frac{1}{8} + \frac{\theta}{4\pi}} \prod_{n=0}^{\infty} \frac{(1 + q^{n+\frac{1}{2}+\frac{\theta}{2\pi}})(1 + q^{n+\frac{1}{2}-\frac{\theta}{2\pi}})}{(1 - q^{n+\frac{\theta}{2\pi}})(1 - q^{n+1-\frac{\theta}{2\pi}})} \right|^2. \tag{4.15}$$

We can now get the θ'-twined character over the θ-twisted sector by acting once more with the orbifold group on the modes. We get the following:

15

$$
\theta' \;\square\; = \operatorname{Tr}_{\mathcal{H}_\theta^{\mathrm{NS}}} \left(U(\theta') q^{L_0 - \frac{1}{8}} \bar{q}^{\bar{L}_0 - \frac{1}{8}} \right)
$$

$$
= \left| q^{-\frac{1}{8} + \frac{\theta}{4\pi}} \prod_{n=0}^{\infty} \frac{(1 + q^{n+\frac{1}{2}+\frac{\theta}{2\pi}} \mathrm{e}^{\mathrm{i}\theta'})(1 + q^{n+\frac{1}{2}-\frac{\theta}{2\pi}} \mathrm{e}^{-\mathrm{i}\theta'})}{(1 - q^{n+\frac{\theta}{2\pi}} \mathrm{e}^{\mathrm{i}\theta'})(1 - q^{n+1-\frac{\theta}{2\pi}} \mathrm{e}^{-\mathrm{i}\theta'})} \right|^2
$$

$$
= \left| \frac{\vartheta_3(\tau, \frac{\tau\theta+\theta'}{2\pi})}{\vartheta_1(\tau, \frac{\tau\theta+\theta'}{2\pi})} \right|^2 , \tag{4.16}
$$

which is the expression we are interested in.

The contribution of a θ-twisted sector to the unprojected partition function is therefore obtained by integrating equation (4.16) over the twisting parameter θ',

$$
\mathcal{P}_{\theta-\mathrm{twisted}}^{\mathrm{NS}} = \frac{1}{2\pi} \int_0^{2\pi} \mathrm{d}\theta' \theta' \;\square\; = \int_0^{2\pi} \frac{\mathrm{d}\theta'}{2\pi} \operatorname{Tr}_{\mathcal{H}_\theta^{\mathrm{NS}}} \left(U(\theta') q^{L_0 - \frac{1}{8}} \bar{q}^{\bar{L}_0 - \frac{1}{8}} \right) \tag{4.17}
$$

$$
= \int_0^{2\pi} \frac{\mathrm{d}\theta'}{2\pi} \left| \frac{\vartheta_3(\tau, \frac{\tau\theta+\theta'}{2\pi})}{\vartheta_1(\tau, \frac{\tau\theta+\theta'}{2\pi})} \right|^2 . \tag{4.18}
$$

Using some identities of appendix C in [24] the modular functions can be recast in the form

$$
\frac{\vartheta_3(\tau, \nu)}{\vartheta_1(\tau, \nu)} = -2\mathrm{i} \frac{\vartheta_3(\tau, 0)}{\eta^3(\tau)} \sum_{n=0}^{\infty} \cos\left[2\pi (n + 1/2)(\nu - \tau/2) \right] \frac{q^{\frac{n}{2}+\frac{1}{4}}}{1 + q^{n+\frac{1}{2}}}, \tag{4.19}
$$

so that the integral (4.18) becomes

$$
\mathcal{P}_{\theta-\mathrm{twisted}}^{\mathrm{NS}} = 4 \left| \frac{\vartheta_3(\tau, 0)}{\eta^3(\tau)} \right|^2 \sum_{n,\bar{n}=0}^{\infty} \frac{q^{\frac{n}{2}+\frac{1}{4}} \bar{q}^{\frac{\bar{n}}{2}+\frac{1}{4}}}{(1 + q^{n+\frac{1}{2}})(1 + \bar{q}^{\bar{n}+\frac{1}{2}})} I_{n,\bar{n}}^\theta \tag{4.20}
$$

with

$$
I_{n,\bar{n}}^\theta = \int_0^{2\pi} \frac{\mathrm{d}\theta'}{2\pi} \cos\left[\left(n + \frac{1}{2} \right) (\tau(\theta - \pi) + \theta') \right] \cos\left[\left(\bar{n} + \frac{1}{2} \right) (\bar{\tau}(\theta - \pi) + \theta') \right] \tag{4.21}
$$

$$
= \frac{\delta_{n,\bar{n}}}{2} \cos\left[\left(n + \frac{1}{2} \right) (\pi - \theta)(\tau - \bar{\tau}) \right]. \tag{4.22}
$$

Inserting (4.22) into (4.20), evaluating the sum over $\bar{n}$, and combining the cosine with the $q, \bar{q}$ dependent part of the numerator, we arrive at

$$
\mathcal{P}_{\theta-\mathrm{twisted}}^{\mathrm{NS}} = \left| \frac{\vartheta_3(\tau, 0)}{\eta^3(\tau)} \right|^2 \sum_{n=0}^{\infty} \frac{q^{\frac{\theta}{2\pi}(n+\frac{1}{2})} \bar{q}^{\frac{\theta}{2\pi}(n+\frac{1}{2})} + q^{(1-\frac{\theta}{2\pi})(n+\frac{1}{2})} \bar{q}^{(1-\frac{\theta}{2\pi})(n+\frac{1}{2})}}{(1 + q^{n+\frac{1}{2}})(1 + \bar{q}^{n+\frac{1}{2}})}. \tag{4.23}
$$

The unprojected supersymmetric partition function is then obtained by integrating over all twisted sectors

$$
\mathcal{P}_{\mathbb{C}/U(1)}^{\mathrm{NS}} = \int_0^{2\pi} \frac{\mathrm{d}\theta}{2\pi} \mathcal{P}_{\theta-\mathrm{twisted}}^{\mathrm{NS}} = \sum_{n=0}^{\infty} \int_{-2\pi}^{2\pi} \frac{\mathrm{d}\theta}{2\pi} \frac{q^{\frac{|\theta|}{2\pi}(n+\frac{1}{2})} \bar{q}^{\frac{|\theta|}{2\pi}(n+\frac{1}{2})}}{(1 + q^{n+\frac{1}{2}})(1 + \bar{q}^{n+\frac{1}{2}})}
$$

$$
= \left| \frac{\vartheta_3(\tau, 0)}{\eta^3(\tau)} \right|^2 \sum_{n=0}^{\infty} \left| \frac{1}{1 + q^{n+\frac{1}{2}}} \right|^2 \int_{-1}^{1} \mathrm{d}Q \, (q\bar{q})^{|Q|(n+\frac{1}{2})}
$$

$$
= \sum_{n=0}^{\infty} \int_{-1}^{1} \mathrm{d}Q \left| \chi_{|Q|(n+\frac{1}{2}),Q}^I \right|^2, \tag{4.24}
$$

where we used the definitions of appendix A for the $c = 3$ character χ^I.

16

The last expression is ill-defined: the integration over Q gives

$$\mathcal{P}^{\mathrm{NS}}_{\mathbb{C}/U(1)} = \frac{1}{2\pi\tau_2} \left| \frac{\vartheta_3(\tau,0)}{\eta^3(\tau)} \right|^2 \sum_{n=0}^{\infty} \frac{1-(q\bar{q})^{n+\frac{1}{2}}}{\left|1+q^{n+\frac{1}{2}}\right|^2} \frac{1}{n+\frac{1}{2}}, \tag{4.25}$$

which exhibits a logarithmic divergence when we sum over n. The fields that contribute to this divergence are the chargeless ones, as one can see by looking at the large n asymptotic behaviour of the function (4.24): the fraction in front of the integral tends to one and the integrand localizes around $Q \sim 0$. Therefore a sensible regulator would screen away the untwisted fields. We define

$$\mathcal{P}^{\mathrm{NS},(r)}_{\mathbb{C}/U(1)} := \left| \frac{\vartheta_3(\tau,0)}{\eta^3(\tau)} \right|^2 \sum_{n=0}^{\infty} \left| \frac{1}{1+q^{n+\frac{1}{2}}} \right|^2 \int_{-1}^{1} \mathrm{d}Q \, (q\bar{q})^{|Q|(n+\frac{1}{2})} \left(1-\mathrm{e}^{2\pi i r Q}\right), \tag{4.26}$$

which corresponds to inserting $1 - \mathrm{e}^{2\pi i r J_0}$ in the trace, where J_0 is the zero mode of the $U(1)$ current $J(z)$. We see explicitly that this cures the logarithmic divergences of the sum in equation (4.24) by performing the integral over the twist Q,

$$\mathcal{P}^{\mathrm{NS},(r)}_{\mathbb{C}/U(1)} = \left| \frac{\vartheta_3(\tau,0)}{\eta^3(\tau)} \right|^2 \sum_{n=0}^{\infty} \left| \frac{1}{1+q^{n+\frac{1}{2}}} \right|^2$$

$$\times \left[\frac{1-(q\bar{q})^{n+\frac{1}{2}}}{2\pi\tau_2(n+\frac{1}{2})} - \frac{1-\mathrm{e}^{2\pi i r}(q\bar{q})^{n+\frac{1}{2}}}{4\pi\tau_2(n+\frac{1}{2}) - 2\pi i r} - \frac{1-\mathrm{e}^{-2\pi i r}(q\bar{q})^{n+\frac{1}{2}}}{4\pi\tau_2(n+\frac{1}{2}) + 2\pi i r} \right]. \tag{4.27}$$

The summand is suppressed by n^{-2} for large n, and the series converges.

From equation (4.26) it is easy to write down the (GSO-like) projected version of the regularized partition function, which reads in the Neveu–Schwarz sector

$$Z^{\mathrm{NS},(r)}_{\mathbb{C}/U(1)} = \frac{1}{2} \left(\left| \frac{\vartheta_3(\tau,0)}{\eta^3(\tau)} \right|^2 + \left| \frac{\vartheta_4(\tau,0)}{\eta^3(\tau)} \right|^2 \right) \sum_{n=0}^{\infty} \left| \frac{1}{1+q^{n+\frac{1}{2}}} \right|^2 \int_{-1}^{1} \mathrm{d}Q \, (q\bar{q})^{|Q|(n+\frac{1}{2})} \left(1-\mathrm{e}^{2\pi i r Q}\right). \tag{4.28}$$

Comparison with the limit of minimal models. We now want to show that the partition function of minimal models reproduces the result of equation (4.28) in the limit we analysed in [8]. We are thus interested in the behaviour of minimal models in the regime in which $n = \frac{l-|m|}{2}$ is a fixed non-negative integer, and $|m|$ scales with k. The Neveu–Schwarz contribution to the partition function for the A_{k+2} minimal model reads (see appendix A for notations and details)

$$Z^{\mathrm{NS}}_k(\tau,\nu) = \frac{1}{2} \sum_{l=0}^{k} \sum_{\substack{m=-l \\ m+l \text{ even}}}^{l} \left[\chi^{\mathrm{NS}}_{l,m} \bar{\chi}^{\mathrm{NS}}_{l,m}(q,z) + \chi^{\mathrm{NS}}_{l,m} \bar{\chi}^{\mathrm{NS}}_{l,m}(q,-z) \right], \tag{4.29}$$

where $z = \mathrm{e}^{2\pi i\nu}$. As before we first analyse the partition function before taking the (GSO-like) projection, i.e. the corresponding trace is taken over the full supersymmetric Hilbert space,

$$\mathcal{P}^{\mathrm{NS}}_k(\tau,\nu) = \sum_{l=0}^{k} \sum_{\substack{m=-l \\ m+l \text{ even}}}^{l} \chi^{\mathrm{NS}}_{l,m} \bar{\chi}^{\mathrm{NS}}_{l,m}(q,z)$$

$$= \left| \frac{\vartheta_3(\tau,\nu)}{\eta^3(\tau)} \right|^2 \sum_{l=0}^{k} \sum_{m=-l}^{l} \left| q^{\frac{(l+1)^2-m^2}{4(k+2)}} \Gamma^{(k)}_{lm}(\tau,\nu) \right|^2. \tag{4.30}$$

For large level k we expect the same kind of divergence as for the partition function of the continuous orbifold due to the almost chargeless field. Similarly to our strategy there we insert the factor $(1 - e^{2\pi i r J_0})$ in the trace, and arrive at (we set $\nu = 0$ in the following)

$$\mathcal{P}_k^{\text{NS},(r)}(\tau) = \left| \frac{\vartheta_3(\tau, 0)}{\eta^3(\tau)} \right|^2 \left[\sum_{n=0}^{\lfloor \frac{k}{2} \rfloor} \mathcal{I}_{k,n}^{(r)} \right] \qquad (4.31)$$

with

$$\mathcal{I}_{k,n}^{(r)} := 2 \sum_{m=1}^{k-2n} (q\bar{q})^{\frac{1}{k+2}\left(n+\frac{1}{2}\right)^2 + \frac{m}{k+2}\left(n+\frac{1}{2}\right)} \left| \Gamma_{m+2n,m}^{(k)}(\tau, 0) \right|^2 \left(1 - \cos\left(2\pi r \frac{m}{k+2}\right) \right). \qquad (4.32)$$

For large level k, the main contribution comes from small n and large m: the regularization factor $(1 - \cos(\cdot))$ is small unless m is of order k, while the exponent containing the conformal weight tells us that for large m only small values of n contribute significantly. In this limit, only one singular vector survives in $\Gamma_{lm}^{(k)}$ (the one present in the $c = 3$ representations of type I in appendix A). Using the Euler–MacLaurin formula to convert the sum over m into an integral, we obtain

$$\mathcal{I}_{k,n}^{(r)} \approx 2 \sum_{m=1}^{k-2n} (q\bar{q})^{\frac{m}{k+2}\left(n+\frac{1}{2}\right)} \left| \frac{1 - q^{m+2n+1}}{(1 + q^{n+\frac{1}{2}})(1 + q^{m+n+\frac{1}{2}})} \right|^2 \left(1 - \cos\left(2\pi r \frac{m}{k+2}\right) \right) \qquad (4.33)$$

$$\approx 2(k+2) \int_0^1 dQ (q\bar{q})^{-Q\left(n+\frac{1}{2}\right)} \left| \frac{1}{(1 + q^{n+\frac{1}{2}})} \right|^2 (1 - \cos(2\pi r Q)). \qquad (4.34)$$

Inserting this into (4.31) and comparing to (4.26) we find

$$\lim_{k \to \infty} \frac{1}{k+2} \mathcal{P}_k^{\text{NS},(r)}(\tau) = \mathcal{P}_{\mathbb{C}/U(1)}^{\text{NS},(r)}(\tau). \qquad (4.35)$$

The rescaling by a factor $1/(k+2)$ can be understood as follows: for a fixed n and a given small interval $[Q, Q + \Delta Q]$ there are roughly $(k+2)\Delta Q$ ground states in the kth minimal model that contribute with approximately the same weight $(q\bar{q})^{|Q|(n+\frac{1}{2})}$. The rescaling thus corresponds to a rescaling of the density of states to 1 per unit interval ΔQ. An analogous relation holds for the true (projected) partition functions, so that indeed we recover the continuous orbifold partition function in the limit.

4.3. Boundary conditions

The technology to study boundary conditions on discrete orbifold models is well developed (see e.g. [26] and references therein), and essentially they are also applicable for the continuous orbifold we are considering (see also [25]).

For continuous orbifolds one meets the phenomenon that the untwisted fields are in a sense outnumbered by the twisted fields—in the partition function (4.28) the untwisted, chargeless fields give a contribution of measure zero. Therefore the only interesting boundary conditions are those that couple to the twisted sectors, i.e. fractional boundary states. To obtain those we have to start from boundary conditions in the plane that are invariant under the action of the orbifold group. In our case, these are the boundary conditions corresponding to a point-like brane at the origin of the plane, and the boundary conditions corresponding to space-filling branes.

Let us focus on the point-like brane. The fractional boundary conditions are then labelled by representations of the orbifold group $U(1)$, i.e. by an integer m. The relative spectrum for two such boundary conditions labelled by m and m' follows from the usual orbifold rules,

$$
\mathcal{P}_{m,m'}(\tilde{q}) = \int_0^{2\pi} \frac{\mathrm{d}\theta}{2\pi} \, \chi_m(\theta)\chi_{m'}^*(\theta) \, \mathrm{Tr}_{\mathcal{H}^{\mathrm{open}}}\left[U(\theta)\tilde{q}^{L_0-\frac{1}{8}}\right], \tag{4.36}
$$

where $\tilde{q} = \mathrm{e}^{2\pi\mathrm{i}\tilde{\tau}}$ and $\chi_m(\theta) = \mathrm{e}^{\mathrm{i}m\theta}$ is a $U(1)$ group character. $\mathcal{H}^{\mathrm{open}}$ denotes the Hilbert space of boundary fields for the point-like brane, which is just given by the free Neveu–Schwarz vacuum representation. Note that depending on the projection of the bulk spectrum, the point-like boundary condition could couple to the Ramond–Ramond sector, in which case the boundary spectrum would be projected by $\frac{1}{2}(1 \pm (-1)^F)$. The unprojected spectrum will be denoted by $\mathcal{P}_{m,m'}$ as introduced above. Evaluating (4.36) we find

$$
\begin{aligned}
\mathcal{P}_{m,m'}(\tilde{q}) &= \int_0^{2\pi} \frac{\mathrm{d}\theta}{2\pi} \mathrm{e}^{\mathrm{i}(m-m')\theta} \, 2\sin\frac{\theta}{2} \, \frac{\vartheta_3(\tilde{\tau}, \frac{\theta}{2\pi})}{\vartheta_1(\tilde{\tau}, \frac{\theta}{2\pi})} \\
&= -4\mathrm{i}\frac{\vartheta_3(\tilde{\tau},0)}{\eta^3(\tilde{\tau})} \sum_{n=0}^{\infty} \frac{q^{\frac{n}{2}+\frac{1}{4}}}{1+q^{n+\frac{1}{2}}} \int_0^{2\pi} \frac{\mathrm{d}\theta}{2\pi} \, \sin\frac{\theta}{2} \, \mathrm{e}^{\mathrm{i}(m-m')\theta} \cos\left(n+\frac{1}{2}\right)(\theta - \pi\tilde{\tau}),
\end{aligned}
\tag{4.37}
$$

where we have made again use of equation (4.19). We can explicitly evaluate the integral,

$$
\begin{aligned}
\int_0^{2\pi} \frac{\mathrm{d}\theta}{2\pi} \, \sin\frac{\theta}{2} \, \mathrm{e}^{\mathrm{i}\Delta m\theta} \cos\left(n+\frac{1}{2}\right)(\theta - \pi\tilde{\tau}) \\
= \frac{1}{4\mathrm{i}}\left[\tilde{q}^{\frac{1}{2}(n+\frac{1}{2})}\left(\delta_{\Delta m,n} - \delta_{\Delta m-1,n}\right) + \tilde{q}^{-\frac{1}{2}(n+\frac{1}{2})}\left(\delta_{-\Delta m+1,n} - \delta_{-\Delta m,n}\right)\right],
\end{aligned}
\tag{4.38}
$$

where $\Delta m = m - m'$. Inserting this into (4.37) we find that the spectrum is given by single $N = 2$ characters: in the notations of appendix A we obtain

$$
\mathcal{P}_{m,m}(\tilde{q}) = \frac{\vartheta_3(\tilde{\tau},0)}{\eta^3(\tilde{\tau})}\left(\frac{1-\tilde{q}^{\frac{1}{2}}}{1+\tilde{q}^{\frac{1}{2}}}\right) = \chi_{0,0}^{\mathrm{vac}}(\tilde{q}) \tag{4.39a}
$$

and (for $m \neq m'$)

$$
\mathcal{P}_{m,m'}(\tilde{q}) = \frac{\vartheta_3(\tilde{\tau},0)}{\eta^3(\tilde{\tau})} \, \tilde{q}^{|\Delta m|-\frac{1}{2}}\left[\frac{1-\tilde{q}}{(1+\tilde{q}^{|\Delta m|-\frac{1}{2}})(1+\tilde{q}^{|\Delta m|+\frac{1}{2}})}\right] = \chi_{|\Delta m|-\frac{1}{2},\pm 1}^{\mathrm{III}^{\pm}}(\tilde{q}), \tag{4.39b}
$$

where the upper sign applies for $\Delta m > 0$ and vice versa. This result can now be compared to the limit of minimal models. In [8] two types of boundary conditions were identified. They arise as limits of A-type boundary conditions in minimal models, which are labelled by triples (L, M, S) with the same range as labels for minimal model fields (see appendix A.2 for the conventions). The first type of boundary conditions is obtained by keeping the boundary labels fixed while taking the limit. Only for $L = 0$ one obtains elementary boundary conditions. The label S can be fixed to even values for a fixed gluing condition for the supercurrents, and the two remaining choices $S = 0, 2$ determine the overall sign of the Ramond–Ramond couplings (thus distinguishing brane and anti-brane). The relative spectrum for two such boundary conditions reads [12]

$$
Z_{(0,M,S),(0,M',S')}^{(k)}(\tilde{q}) = \chi_{(0,M-M',S-S'+2)}(\tilde{q}). \tag{4.40}
$$

This is a projected part of the full supersymmetric character $\chi_{0,M-M'}^{\mathrm{NS}}$. For $M = M'$ this is the minimal model vacuum character, which for $k \to \infty$ goes to the $c = 3$ vacuum character. For $M \neq M'$, using field identification (see (A.11)) the labels can be brought to the standard range,

$(0, M - M') \sim (k, M - M' \mp (k + 2))$, where the sign depends on $M - M'$ being positive or negative. In the limit $k \to \infty$ the corresponding character approaches a type III character (see (A.21) and (A.22)),

$$\lim_{k\to\infty} \chi^{\text{NS}}_{0,M-M'\mp(k+2)} = \chi^{\text{III}^\pm}_{\frac{M-M'}{2}-\frac{1}{2},\pm 1}. \tag{4.41}$$

The unprojected part of the boundary spectrum thus coincides with the spectrum for the fractional boundary conditions in the continuous orbifold upon identifying $M = 2m$. On the other hand, the spectrum in the limit of minimal models is projected. To get agreement we therefore need that the point-like boundary conditions in the continuous orbifold model couple to the Ramond–Ramond sector, which specifies the necessary (GSO-like) projection in the Ramond–Ramond sector. Note that this is precisely opposite from the projection that we need in the free field theory limit, which is in accordance with the T-duality that we use in the geometric interpretation of the equivalence of a minimal model and its $\mathbb{Z}_{k+2}$ orbifold (see the discussion at the end of section 2).

In [8], instead of the boundary spectrum, the one-point functions have been determined. To make contact to these results, we perform a modular transformation to get the boundary state overlap: we rewrite the boundary partition function (4.37) in terms of the modulus $\tau = -\frac{1}{\tilde\tau}$ using the known transformation properties (4.13),

$$\mathcal{P}_{m,m'}(\tilde q) = 2i \int_0^{2\pi} \frac{d\theta}{2\pi} e^{i(m-m')\theta} \sin\frac{\theta}{2} \frac{\vartheta_3(\tau, \frac{\tau\theta}{2\pi})}{\vartheta_1(\tau, \frac{\tau\theta}{2\pi})}. \tag{4.42}$$

The ratio of ϑ-functions can be rewritten using equation (4.19),

$$\begin{aligned}
\frac{\vartheta_3\left(\tau, \frac{\tau\theta}{2\pi}\right)}{\vartheta_1\left(\tau, \frac{\tau\theta}{2\pi}\right)} &= -2i \frac{\vartheta_3(\tau,0)}{\eta^3(\tau)} \sum_{n=0}^{\infty} \cos\left[2\pi(n+1/2)\left(\frac{\tau\theta}{2\pi} - \tau/2\right)\right] \frac{q^{\frac{n}{2}+\frac{1}{4}}}{1+q^{n+\frac{1}{2}}} \\
&= -i \frac{\vartheta_3(\tau,0)}{\eta^3(\tau)} \sum_{n=0}^{\infty} \frac{q^{(n+\frac{1}{2})\frac{\theta}{2\pi}} + q^{(n+\frac{1}{2})(1-\frac{\theta}{2\pi})}}{1+q^{n+\frac{1}{2}}},
\end{aligned} \tag{4.43}$$

so that we obtain

$$\begin{aligned}
\mathcal{P}_{m,m'}(\tilde q) &= \frac{\vartheta_3(\tau,0)}{\eta^3(\tau)} \int_0^{2\pi} \frac{d\theta}{2\pi} e^{i(m-m')\theta} \, 2\sin\frac{\theta}{2} \sum_{n=0}^{\infty} \frac{q^{(n+\frac{1}{2})\frac{\theta}{2\pi}} + q^{(n+\frac{1}{2})(1-\frac{\theta}{2\pi})}}{1+q^{n+\frac{1}{2}}} \\
&= \sum_{n=0}^{\infty} \int_{-1}^{+1} dQ \, 2\sin(\pi|Q|) \, e^{2\pi i(m-m')Q} \, \chi^I_{|Q|(n+\frac{1}{2}),Q}(q).
\end{aligned} \tag{4.44}$$

If we do the same analysis for the projected spectrum, we find

$$\begin{aligned}
Z_{m,m'}(\tilde q) &= \sum_{n=0}^{\infty} \int_{-1}^{+1} dQ \, \sin(\pi|Q|) \, e^{2\pi i(m-m')Q} \left(\chi^{\text{NS}}_{|Q|(n+\frac{1}{2}),Q}(q) + \chi^{\text{R}}_{\frac{1}{8}+|Q|(n+1),Q}(q) \right) \\
&\quad + \int_{-\frac{1}{2}}^{\frac{1}{2}} dQ \, \sin\left(\pi\left|Q - \frac{1}{2}\right|\right) e^{2\pi i(m-m')(Q-\frac{1}{2})} \chi^{\text{R}^0}_{\frac{1}{8},Q}(q).
\end{aligned} \tag{4.45}$$

Comparing with the formulae presented in reference [8, equations (4.5)–(4.7)], we find perfect agreement with the one-point functions given there for the discrete A-type boundary states of the limit theory for $L = 0$ and with the identification $M = 2m$.

Along similar lines let us briefly discuss boundary conditions that correspond to two-dimensional branes. As we discussed at the end of section 3.5, there is a one-parameter family of those that differ in the strength of a constant electric background field, which can be labelled by an angle ϕ. In the orbifold the boundary conditions obtain an additional integer label m that determines the corresponding representation of $U(1)$. The unprojected part of the annulus

partition function with such a two-dimensional boundary condition labelled by ϕ and m, and a zero-dimensional boundary condition labelled by m' is then (using again (4.19))

$$\mathcal{P}_{(\phi,m),m'}(\tilde{q}) = \int_0^{2\pi} \frac{\mathrm{d}\theta}{2\pi} \, \mathrm{e}^{\mathrm{i}(m-m'+\frac{1}{2})\theta} \mathrm{i} \frac{\vartheta_3 \left(\tilde{\tau}, \frac{\theta+(\phi+\pi)\tilde{\tau}}{2\pi} \right)}{\vartheta_1 \left(\tilde{\tau}, \frac{\theta+(\phi+\pi)\tilde{\tau}}{2\pi} \right)} \tag{4.46}$$

$$= \frac{\vartheta_3(\tilde{\tau}, 0)}{\eta^3(\tilde{\tau})} \frac{\tilde{q}^{\frac{\pi \mp \phi}{2\pi} |\Delta m + \frac{1}{2}|}}{1 + \tilde{q}^{|\Delta m + \frac{1}{2}|}}, \tag{4.47}$$

where the upper sign corresponds to $\Delta m = m - m' \geqslant 0$, and the lower one to $\Delta m < 0$. These are the type I characters $\chi^{I^{\pm}}_{(n+\frac{1}{2})|Q|,Q}$ for charge $|Q| = \frac{\pi \mp \phi}{2\pi}$ and $n = |\Delta m + \frac{1}{2}| - \frac{1}{2}$. Note that this is precisely the result we expect from the limit of minimal models: in [8] we constructed a continuous family of A-type boundary states labelled by Q, N as a limit of minimal model boundary states with labels

$$(L, M, S) = (|\lfloor -Q(k+2) \rfloor| + 2N, \lfloor -Q(k+2) \rfloor, 0), \tag{4.48}$$

where $\lfloor x \rfloor$ denotes the greatest integer smaller or equal x. Their relative spectrum (without projection) to a boundary condition $(0, M', 0)$ with fixed M' is simply given by $\chi^{\mathrm{NS}}_{L,M-M'}$, and in the limit we find (see appendix A.3)

$$\chi^{\mathrm{NS}}_{|\lfloor -Q(k+2) \rfloor|+2N, \lfloor -Q(k+2) \rfloor - M'} \rightarrow \begin{cases} \chi^{I^+}_{|Q| \left| N - \frac{M'}{2} + \frac{1}{2} \right|, Q} & Q > 0, \ N \geqslant \frac{M'}{2} \\ \chi^{I^+}_{|Q-1| \left| N - \frac{M'}{2} + \frac{1}{2} \right|, Q-1} & Q > 0, \ N < \frac{M'}{2} \\ \chi^{I^-}_{|Q| \left| N + \frac{M'}{2} + \frac{1}{2} \right|, Q} & Q < 0, \ N \geqslant -\frac{M'}{2} \\ \chi^{I^-}_{|Q+1| \left| N + \frac{M'}{2} + \frac{1}{2} \right|, Q+1} & Q < 0, \ N < -\frac{M'}{2} \end{cases} . \tag{4.49}$$

These are the type I characters that we found above in (4.47) if we identify

$$\phi = 2\pi \left(-Q \pm \frac{1}{2} \right), m = -\frac{1}{2} \pm \left(N + \frac{1}{2} \right), \tag{4.50}$$

where the upper sign applies for $Q > 0$, and the lower for $Q < 0$.

5. Discussion

We have shown that one can obtain two different limits of the sequence of $N = (2, 2)$ minimal models, and we have discussed how these limits can be understood geometrically. The first limit theory is simply a free field theory, the second limit theory is the non-rational theory of [8], and we have shown that it can be described as a continuous orbifold $\mathbb{C}/U(1)$. The latter observation is reminiscent of the recent interpretation of the limit of Virasoro minimal models as a continuous orbifold $SU(2)_1/SO(3)$ [25].

It would be interesting to explore similar limits in the case of other series of $N = (2, 2)$ superconformal models, like the Grassmannian Kazama–Suzuki models [27] based on $SU(n + 1)/U(n)$. Again one might expect to find different possible limit theories; in fact there might be a greater variety of limits, because in addition to the $U(1)$ charge there are charges associated to currents of higher spin for which one might have the freedom to scale them while taking the limit. One is tempted to speculate that the limit theory corresponding to fixed charges is again described by a continuous orbifold $\mathbb{C}^n/U(n)$. It would be interesting to study this in detail. This could also be of relevance in the context of the supersymmetric

generalization of minimal model holography [28, 29], where a limit of Kazama–Suzuki models occurs in the conjectured holographic dual of supersymmetric higher-spin theories on three-dimensional asymptotically anti-de Sitter space-times [30–34].

Acknowledgments

Appendix A. Characters

In this appendix we collect results about characters for $N = 2$ theories and their limits. A general character over a sector $\mathcal{H}_{h,Q}$ labelled by h, Q (eigenvalues of the L_0, J_0 generators respectively) of the $N = 2$ superconformal algebra is defined as

$$\chi_{h,Q}(q, z) = \mathrm{Tr}_{\mathcal{H}_{h,Q}} q^{L_0 - \frac{c}{24}} z^{J_0}, \tag{A.1}$$

with $q = \mathrm{e}^{2\pi i \tau}$, $z = \mathrm{e}^{2\pi i \nu}$. In the main text we often make use of the following shorthand notation for characters specialized to $z = 1$,

$$\chi_{h,Q}(q) \equiv \chi_{h,Q}(q, 1). \tag{A.2}$$

Throughout the text we use ϑ and η functions with the following conventions:

$$\vartheta_1(\tau, \nu) = -\mathrm{i} z^{\frac{1}{2}} q^{\frac{1}{8}} \prod_{n=0}^{\infty} (1 - q^{n+1}z)(1 - q^n z^{-1})(1 - q^{n+1}),$$

$$\vartheta_2(\tau, \nu) = z^{\frac{1}{2}} q^{\frac{1}{8}} \prod_{n=0}^{\infty} (1 + q^{n+1}z)(1 + q^n z^{-1})(1 - q^{n+1}),$$

$$\vartheta_3(\tau, \nu) = \prod_{n=0}^{\infty} (1 + q^{n+\frac{1}{2}}z)(1 + q^{n+\frac{1}{2}} z^{-1})(1 - q^{n+1}),$$

$$\vartheta_4(\tau, \nu) = \prod_{n=0}^{\infty} (1 - q^{n+\frac{1}{2}}z)(1 - q^{n+\frac{1}{2}} z^{-1})(1 - q^{n+1}),$$

$$\eta(\tau) = q^{\frac{1}{24}} \prod_{n=0}^{\infty} (1 - q^{n+1}).$$

A.1. $c = 3$ characters

We discuss here the characters of the unitary fully supersymmetric irreducible representations of the $N = 2$ superconformal algebra at $c = 3$. The Verma modules of the $N = 2$ superconformal algebra contain several singular submodules[8], which have to be taken into account. The structure of the singular submodules can be read off from the embedding diagrams of the representations (for further details we refer to [36, 37]); we will follow the classification of [35]. Let us explain the procedure at the example of the characters for the representations of type $I^{\pm}$ in the notations of the aforementioned paper; the labels satisfy $\frac{h}{Q} \in \mathbb{Z} + \frac{1}{2}$, with

---

[8] In general there are also subsingular submodules, but they do not show up for unitary representations [35].

positive h and $Q \notin \mathbb{Z}$. In this case we have only one charged singular vector. The singular vectors at level $\frac{h}{|Q|} = n + \frac{1}{2}$ can be recognized to be[9]

$$
\begin{aligned}
G_{\frac{1}{2}}^- G_{\frac{3}{2}}^- \ldots G_{-\frac{h}{|Q|}-1}^- G_{-\frac{h}{|Q|}}^+ G_{-\frac{h}{|Q|}+1}^+ \ldots G_{-\frac{3}{2}}^+ G_{-\frac{1}{2}}^+ |n, Q\rangle, \quad \text{for} \quad Q > 0 \\
G_{\frac{1}{2}}^+ G_{\frac{3}{2}}^+ \ldots G_{-\frac{h}{|Q|}-1}^+ G_{-\frac{h}{|Q|}}^- G_{-\frac{h}{|Q|}+1}^- \ldots G_{-\frac{3}{2}}^- G_{-\frac{1}{2}}^- |n, Q\rangle, \quad \text{for} \quad Q < 0
\end{aligned}
$$
(A.3)

and they have relative charge $+1$ and -1, respectively. Here, $G_r^{\pm}$ denote the modes of the supercurrents of the $N = 2$ superconformal algebra. In the character of the irreducible representation we have to subtract the contribution of the submodule associated to them. The result is

$$
\chi_{n,Q}^{I^{\pm}}(q, z) = q^{(n+\frac{1}{2})|Q|-\frac{1}{8}} z^Q \left[\prod_{m=0}^{\infty} \frac{(1 + q^{m+\frac{1}{2}}z)(1 + q^{m+\frac{1}{2}}z^{-1})}{(1 - q^{m+1})^2} \right] \left(1 - \frac{q^{n+\frac{1}{2}}z^{\mathrm{sgn}Q}}{1 + q^{n+\frac{1}{2}}z^{\mathrm{sgn}Q}} \right). \quad \text{(A.4)}
$$

The other cases are analogous, and we can write:

- vacuum: $(Q = h = 0)$

$$
\chi_{0,0}^{\mathrm{vac}}(q, z) = \frac{\vartheta_3(\tau, \nu)}{\eta^3(\tau)} \left(1 - \frac{q^{\frac{1}{2}}z}{1 + q^{\frac{1}{2}}z} - \frac{q^{\frac{1}{2}}z^{-1}}{1 + q^{\frac{1}{2}}z^{-1}} \right); \quad \text{(A.5a)}
$$

- type 0: $(Q = 0, \ h \in \mathbb{R} \setminus \{0\})$

$$
\chi_{h,0}^0(q, z) = q^h \frac{\vartheta_3(\tau, \nu)}{\eta^3(\tau)}; \quad \text{(A.5b)}
$$

- type I$^{\pm}$: $(0 < |Q| < 1, \ h = |Q|(n + \frac{1}{2}), \ n \in \mathbb{Z}_{\geqslant 0})$

$$
\chi_{|Q|(n+\frac{1}{2}),Q}^{I^{\pm}}(q, z) = q^{(n+\frac{1}{2})|Q|} z^Q \frac{\vartheta_3(\tau, \nu)}{\eta^3(\tau)} \left(1 - \frac{q^{n+\frac{1}{2}}z^{\mathrm{sgn}Q}}{1 + q^{n+\frac{1}{2}}z^{\mathrm{sgn}Q}} \right); \quad \text{(A.5c)}
$$

- type II$^{\pm}$: $(Q = \pm 1, \ h \in \mathbb{R}_{\geqslant 0})$

$$
\chi_{h,Q}^{II^{\pm}}(q, z) = q^h z^Q \frac{\vartheta_3(\tau, \nu)}{\eta^3(\tau)} \left(1 - q^{|Q|} \right); \quad \text{(A.5d)}
$$

- type III$^{\pm}$: $(Q = \pm 1, \ h \in \mathbb{Z} + \frac{1}{2})$

$$
\chi_{h,Q}^{III^{\pm}}(q, z) = q^h z^Q \frac{\vartheta_3(\tau, \nu)}{\eta^3(\tau)} \left(1 - q - \frac{q^h z^{\mathrm{sgn}(Q)}}{1 + q^h z^{\mathrm{sgn}(Q)}} + \frac{q^{h+2} z^{\mathrm{sgn}(Q)}}{1 + q^{h+1} z^{\mathrm{sgn}(Q)}} \right). \quad \text{(A.5e)}
$$

Ramond characters can be obtained from the Neveu–Schwarz characters by spectral flow (see e.g. [38]). We give an example: let us denote spectral flowed operators and sectors by an upper label η, which indicates the amount of spectral flow units to use. Under a flow of $\eta = \pm 1/2$, primary vectors of the Neveu–Schwarz sector become Ramond primaries, and the same happens for Neveu–Schwarz singular vectors, which flow to Ramond singular vectors. The Ramond characters can then be computed using the formula

$$
\chi_{h^\eta, Q^\eta}(q, z) = \mathrm{Tr}_{\mathcal{H}_{h^\eta, Q^\eta}} q^{L_0 - \frac{c}{24}} z^{J_0} = \mathrm{Tr}_{\mathcal{H}_{h,Q}} q^{L_0^\eta - \frac{c}{24}} z^{J_0^\eta}, \quad \text{(A.6)}
$$

with the spectral flowed operators

$$
L_n^\eta = L_n - \eta J_n + \frac{c}{6} \eta^2 \delta_{n,0}, \qquad J_n^\eta = J_n - \frac{c}{3} \eta \delta_{n,0}. \quad \text{(A.7)}
$$

---

[9] One can, for instance, follow the spectral flow of Neveu–Schwarz null vectors starting from the (anti)chiral primaries.

For $c = 3$ and $\eta = \frac{1}{2}$, $L_0^{1/2} = L_0 - \frac{1}{2}J_0 + \frac{1}{8}$ and $J_0^{1/2} = J_0 - \frac{1}{2}$, we have

$$\chi_{h^{1/2},Q^{1/2}}(q,z) = q^{\frac{1}{8}} z^{-\frac{1}{2}} \chi_{h,Q}(q, q^{-\frac{1}{2}} z). \tag{A.8}$$

Starting, e.g., from the type I characters in the Neveu–Schwarz sector we find the characters

$$\chi_{\frac{1}{8},Q}^{R^0}(q,z) = \frac{z^Q}{z^{1/2} - z^{-1/2}} \frac{\vartheta_2(\tau,\nu)}{\eta^3(\tau)}, \qquad -\frac{1}{2} < Q < \frac{1}{2}, \tag{A.9}$$

$$\chi_{\frac{1}{8}+n|Q|,Q}^{R}(q,z) = \frac{q^{n|Q|} z^Q}{1 + q^n z^{\mathrm{sgn}(Q)}} \frac{\vartheta_2(\tau,\nu)}{\eta^3(\tau)}, \qquad 0 < |Q| < 1, \quad n \geqslant 1, \tag{A.10}$$

where in the first character the lowest lying state is a Ramond ground state, whereas in the second character there are two lowest lying states of charges $Q \pm \frac{1}{2}$.

A.2. Minimal model characters and partition function

Unitary irreducible representations for the bosonic subalgebra of the $N = 2$ superconformal algebra at central charge $c = 3\frac{k}{k+2}$ are labelled by three integers (l, m, s) with $0 \leqslant l \leqslant k$, $m \equiv m+2k+4$, $s \equiv s+4$, and $l+m+s$ even. Not all triples label independent representations, and they are identified according to

$$(l, m, s) \sim (k - l, m + k + 2, s + 2). \tag{A.11}$$

Representations of the full superconformal algebra are then obtained by combining representations labelled by (l, m, s) and $(l, m, s + 2)$.

Explicit expressions for the characters of the $N = 2$ superconformal algebra can be found e.g. in [39]. In the Neveu–Schwarz sector for $|m| \leqslant l$ they read

$$\chi_{l,m}^{NS}(q,z) := \left(\chi_{(l,m,0)} + \chi_{(l,m,2)}\right)(q,z)$$
$$= q^{\frac{(l+1)^2-m^2}{4(k+2)} - \frac{1}{8}} z^{-\frac{m}{k+2}} \left[\prod_{n=0}^{\infty} \frac{(1+q^{n+\frac{1}{2}}z)(1+q^{n+\frac{1}{2}}z^{-1})}{(1-q^{n+1})^2}\right] \times \Gamma_{lm}^{(k)}(\tau,\nu), \tag{A.12}$$

and in the Ramond sector (for $|m| \leqslant l + 1$)

$$\chi_{l,m}^{R}(q,z) := \left(\chi_{(l,m,1)} + \chi_{(l,m,-1)}\right)(q,z)$$
$$= q^{\frac{(l+1)^2-m^2}{4(k+2)}} z^{-\frac{m}{k+2}} (z^{\frac{1}{2}} + z^{-\frac{1}{2}}) \left[\prod_{n=0}^{\infty} \frac{(1+q^{n+1}z)(1+q^{n+1}z^{-1})}{(1-q^{n+1})^2}\right] \times \Gamma_{lm}^{(k)}(\tau,\nu), \tag{A.13}$$

where the structure of the singular vectors is summarized in $\Gamma_{lm}^{(k)}$,

$$\Gamma_{lm}^{(k)}(\tau,\nu) = \sum_{p=0}^{\infty} q^{(k+2)p^2+(l+1)p} \left(1 - \frac{q^{(k+2)p+\frac{l+m+1}{2}}z}{1+q^{(k+2)p+\frac{l+m+1}{2}}z} - \frac{q^{(k+2)p+\frac{l-m+1}{2}}z^{-1}}{1+q^{(k+2)p+\frac{l-m+1}{2}}z^{-1}}\right)$$
$$- \sum_{p=1}^{\infty} q^{(k+2)p^2-(l+1)p} \left(1 - \frac{q^{(k+2)p-\frac{l+m+1}{2}}z^{-1}}{1+q^{(k+2)p-\frac{l+m+1}{2}}z^{-1}} - \frac{q^{(k+2)p-\frac{l-m+1}{2}}z}{1+q^{(k+2)p-\frac{l-m+1}{2}}z}\right). \tag{A.14}$$

The Neveu–Schwarz part of the minimal model partition function is given by

$$Z_k^{NS}(\tau,\nu) = \sum_{l=0}^{k} \sum_{\substack{m=-l \\ l+m \text{ even}}}^{l} \chi_{(l,m,0)}(q,z)\bar{\chi}_{(l,m,0)}(\bar{q},\bar{z}) + \chi_{(l,m,2)}(q,z)\bar{\chi}_{(l,m,2)}(\bar{q},\bar{z})$$

$$= \frac{1}{2} \sum_{l=0}^{k} \sum_{\substack{m=-l \\ l+m \text{ even}}}^{l} \left(\chi_{l,m}^{NS}(q,z)\bar{\chi}_{l,m}^{NS}(\bar{q},\bar{z}) + \chi_{l,m}^{NS}(q,-z)\bar{\chi}_{l,m}^{NS}(\bar{q},-\bar{z})\right). \tag{A.15}$$

It can be seen as a (GSO-like) projection of the trace over the full supersymmetric Neveu–Schwarz Hilbert space $\mathcal{H}_k^{\mathrm{NS}} = \oplus_{|m| \leqslant l \leqslant k} \mathcal{H}_{l,m}^{\mathrm{NS}} \otimes \mathcal{H}_{l,m}^{\mathrm{NS}}$,

$$
\mathcal{P}_k^{\mathrm{NS}}(\tau, \nu) := \sum_{l=0}^{k} \sum_{\substack{m=-l \\ l+m \text{ even}}}^{l} \left(\chi_{(l,m,0)}(q,z) + \chi_{(l,m,2)(q,z)} \right) \left(\bar{\chi}_{(l,m,0)}(\bar{q}, \bar{z}) + \bar{\chi}_{(l,m,2)(\bar{q},\bar{z})} \right)
$$

$$
= \left| \frac{\vartheta_3(\tau, \nu)}{\eta^3(\tau)} \right|^2 \sum_{l=0}^{k} \sum_{\substack{m=-l \\ l+m \text{ even}}}^{l} \left| q^{\frac{(l+1)^2 - m^2}{4(k+2)}} \Gamma_{lm}^{(k)}(\tau, \nu) \right|^2 (z\bar{z})^{-\frac{m}{k+2}} . \tag{A.16}
$$

A.3. Limit of minimal model characters

In the limit $k \to \infty$ in the expression (A.14) for $\Gamma_{lm}^{(k)}$ in each sum only the first summand can contribute,

$$
\Gamma_{lm}^{(k)}(\tau, \nu) \approx \left(1 - \frac{q^{\frac{l+m+1}{2}} z}{1 + q^{\frac{l+m+1}{2}} z} - \frac{q^{\frac{l-m+1}{2}} z^{-1}}{1 + q^{\frac{l-m+1}{2}} z^{-1}} \right)
$$

$$
- q^{k-l+1} \left(1 - \frac{q^{\frac{2k-l-m+3}{2}} z^{-1}}{1 + q^{\frac{2k-l-m+3}{2}} z^{-1}} - \frac{q^{\frac{2k-l+m+3}{2}} z}{1 + q^{\frac{2k-l+m+3}{2}} z} \right), \tag{A.17}
$$

and the precise behaviour of the character depends on the details of how l and m behave in the limit.

For our analysis we need to consider the following cases in the Neveu–Schwarz sector:

(1) $l = m = 0$: the limit character is simply the $N = 2$ vacuum character,

$$
\lim_{k \to \infty} \chi_{0,0}^{\mathrm{NS}} = \chi_{0,0}^{\mathrm{vac}} . \tag{A.18}
$$

(2) $l + m = 2n$ finite, $m/(k+2) \to -Q$, $0 < Q < 1$: only one singular vector survives and we find

$$
\lim_{k \to \infty} \chi_{|m|+2n,m}^{\mathrm{NS}} = \chi_{Q(n+\frac{1}{2}),Q}^{I^+} . \tag{A.19}
$$

(3) $l - m = 2n$ finite, $m/(k+2) \to -Q$, $-1 < Q < 0$: only one singular vector survives and we find

$$
\lim_{k \to \infty} \chi_{m+2n,m}^{\mathrm{NS}} = \chi_{|Q|(n+\frac{1}{2}),Q}^{I^-} . \tag{A.20}
$$

(4) $l + m = 2n$ finite, $l = k$: the first summand in (A.17) gives one positively charged singular vector, the second produces one uncharged one and adds one positively charged singular submodule. We find

$$
\lim_{k \to \infty} \chi_{k,-k+2n}^{\mathrm{NS}} = \chi_{n+\frac{1}{2},1}^{\mathrm{III}^+} . \tag{A.21}
$$

(5) $l - m = 2n$ finite, $l = k$: analogously to the previous case we obtain

$$
\lim_{k \to \infty} \chi_{k,k-2n}^{\mathrm{NS}} = \chi_{n+\frac{1}{2},-1}^{\mathrm{III}^-} . \tag{A.22}
$$

There are several other cases, depending on the behaviour of $l \pm m$ for large k; in these other situations the limiting character decomposes into a sum of $N = 2$ characters. We illustrate this in the example of fixed labels l, m: in this instance the conformal weights and $U(1)$ charge of all the primary fields approach zero, the second line of equation (A.17) gets suppressed, but the first line stays finite. The character then takes the form

$$\lim_{k\to\infty} \chi_{l,m}^{\mathrm{NS}}(q,z) = \frac{\vartheta_3(\tau,\nu)}{\eta^3(\tau)} \left(1 - \frac{q^{\frac{l+m+1}{2}} z}{1 + q^{\frac{l+m+1}{2}} z} - \frac{q^{\frac{l-m+1}{2}} z^{-1}}{1 + q^{\frac{l-m+1}{2}} z^{-1}} \right). \quad (A.23)$$

Noticing the relation

$$\frac{\vartheta_3(\tau,\nu)}{\eta^3(\tau)} \left(\frac{q^{n+\frac{1}{2}} z^{\pm 1}}{1 + q^{n+\frac{1}{2}} z^{\pm 1}} - \frac{q^{n+\frac{3}{2}} z^{\pm 1}}{1 + q^{n+\frac{3}{2}} z^{\pm 1}} \right) = \chi_{n+\frac{1}{2},\pm 1}^{\mathrm{III}\pm}(q,z), \quad (A.24)$$

it is easy to show that

$$\lim_{k\to\infty} \chi_{l,m}^{\mathrm{NS}} = \chi_{0,0}^{\mathrm{vac}} + \sum_{j=0}^{\frac{l+m}{2}-1} \chi_{\frac{l+m}{2}-(\frac{1}{2}+j),1}^{\mathrm{III}+} + \sum_{j=0}^{\frac{l-m}{2}-1} \chi_{\frac{l-m}{2}-(\frac{1}{2}+j),-1}^{\mathrm{III}-}. \quad (A.25)$$

Following similar lines it is possible to show that this kind of decomposition is common to all the cases we have not listed explicitly.

Appendix B. Asymptotics of Wigner 3j-symbols

We are interested in the region of the parameter space of $3j$-symbols in which the angular momentum labels j_i scale like $j_i \propto \sqrt{k}$ and the magnetic labels μ_i stay finite in the limit of large k. In this range we are deeply inside the classically allowed region (see e.g. the appendix A of [8] for more details), and we can use the approximation methods derived in [40]. In particular we find there [40, equation (3.23)]

$$\begin{pmatrix} j_1 & j_2 & j_3 \\ \mu_1 & \mu_2 & \mu_3 \end{pmatrix} \simeq 2 I_{j_1 \mu_1 j_2 \mu_2 j_3 \mu_3} (-1)^{j_1 - j_2 - \mu_3} \sqrt{\frac{j_3}{2j_3 + 1}} \frac{\cos\left[\chi + \frac{\pi}{4} - \pi(j_3 + 1)\right]}{(4\pi A(\lambda_1, \lambda_2, \lambda_2))^{1/2}}, \quad (B.1)$$

where χ is defined as

$$\chi = \left(j_1 + \frac{1}{2}\right)\gamma_1 + \left(j_2 + \frac{1}{2}\right)\gamma_2 + \left(j_3 + \frac{1}{2}\right)\gamma_3 + \mu_2 \beta_1 - \mu_1 \beta_2. \quad (B.2)$$

We use the Ponzano–Regge angles $\gamma_{1,2,3}, \beta_{1,2}$ (see [41] and figure B1) which through their cosines read

$$\cos\gamma_1 = \frac{\mu_3(j_1^2 + j_2^2 - j_3^2) - \mu_2(j_1^2 + j_3^2 - j_2^2)}{4A(j_1, j_2, j_3)\lambda_1}, \quad \cos\beta_1 = \frac{\lambda_3^2 + \lambda_2^2 - \lambda_1^2}{2\lambda_2\lambda_3}, \quad (B.3a)$$

$$\cos\gamma_2 = \frac{\mu_1(j_3^2 + j_2^2 - j_1^2) - \mu_3(j_2^2 + j_1^2 - j_3^2)}{4A(j_1, j_2, j_3)\lambda_2}, \quad \cos\beta_2 = \frac{\lambda_1^2 + \lambda_3^2 - \lambda_2^2}{2\lambda_1\lambda_3}, \quad (B.3b)$$

$$\cos\gamma_3 = \frac{\mu_2(j_1^2 + j_3^2 - j_2^2) - \mu_1(j_3^2 + j_2^2 - j_1^2)}{4A(j_1, j_2, j_3)\lambda_3}. \quad (B.3c)$$

Here,

$$\lambda_i = \sqrt{j_i^2 - \mu_i^2}, \qquad i = 1, 2, 3, \quad (B.4)$$

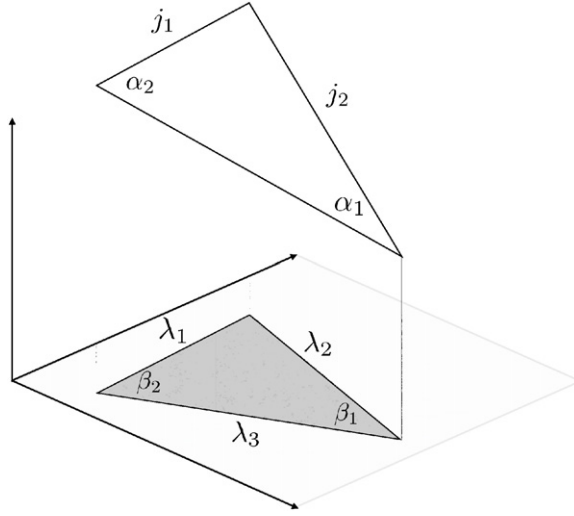**Figure B1.** Ponzano–Regge angles defined in equations (B.3) and (B.13): the α_i are the internal angles of the triangle formed by the j_i labels; the β_i are the internal angles of the triangle projected on the xy-plane (where the μ_i measure the z-components of the angular momenta); γ_i (not present here) is the angle between the outer normals to the faces adjacent to the edge j_i.

and

$$A(x_1, x_2, x_3) = \tfrac{1}{4}\sqrt{(x_3 + x_1 + x_2)(-x_3 + x_1 + x_2)(x_3 - x_1 + x_2)(x_3 + x_1 - x_2)} \tag{B.5}$$

is the area of the triangle with side lengths x_i.

The quantity $I_{j_1 \mu_1 j_2 \mu_2 j_3 \mu_3}$ appearing in equation (B.1) is defined as

$$
\begin{aligned}
I_{j_1 \mu_1 j_2 \mu_2 j_3 \mu_3} =\ & \sqrt{\frac{(j_3 + 1/2)(j_3 + j_1 + j_2)}{j_3 (j_3 + j_1 + j_2 + 1)}} \\
& \times \frac{f(j_1 + \mu_1)f(j_1 - \mu_1)f(j_2 + \mu_2)f(j_2 - \mu_2)f(j_3 + \mu_3)f(j_3 - \mu_3)}{f(j_1 + j_2 + j_3)f(j_1 + j_2 - j_3)f(j_1 - j_2 + j_3)f(-j_1 + j_2 + j_3)},
\end{aligned}
\tag{B.6}
$$

where $f(n)$ is the square root of the ratio of $n!$ to the Stirling approximation of $n!$, and has the following large n behaviour:

$$f(n) = \sqrt{\frac{n!}{\sqrt{2\pi n}\, n^n \mathrm{e}^{-n}}} = 1 + \frac{1}{24n} + \mathcal{O}\left(\frac{1}{n^2}\right). \tag{B.7}$$

We now consider the situation where the labels j_i are proportional to $\sqrt{k}$ for large k while keeping μ_i finite. In this regime we have

$$I = 1 + \mathcal{O}\left(k^{-1/2}\right), \tag{B.8}$$

and the angles behave as follows:

$$\cos \gamma_{1,2,3} = f_{1,2,3} + \mathcal{O}(k^{-3/2}), \tag{B.9a}$$

$$\cos \beta_1 = \frac{-j_1^2 + j_2^2 + j_3^2}{2 j_2 j_3} + \mathcal{O}(k^{-1}), \quad \cos \beta_2 = \frac{j_1^2 - j_2^2 + j_3^2}{2 j_1 j_3} + \mathcal{O}(k^{-1}), \tag{B.9b}$$

where we used the definitions

$$f_1 = \frac{\mu_3(j_1^2 + j_2^2 - j_3^2) - \mu_2(j_1^2 - j_2^2 + j_3^2)}{4A(j_1, j_2, j_3)j_1} \propto k^{-\frac{1}{2}}, \tag{B.10a}$$

$$f_2 = \frac{\mu_1(-j_1^2 + j_2^2 + j_3^2) - \mu_3(j_1^2 + j_2^2 - j_3^2)}{4A(j_1, j_2, j_3)j_2} \propto k^{-\frac{1}{2}}, \tag{B.10b}$$

$$f_3 = \frac{\mu_2(j_1^2 - j_2^2 + j_3^2) - \mu_1(-j_1^2 + j_2^2 + j_3^2)}{4A(j_1, j_2, j_3)j_3} \propto k^{-\frac{1}{2}}. \tag{B.10c}$$

Inverting (B.3) and expanding in k we get $\gamma_{1,2,3} = \frac{\pi}{2} - \frac{f_{1,2,3}}{k^{1/2}} + \mathcal{O}(k^{-3/2})$, so that χ of equation (B.2) becomes

$$\chi = \frac{\pi}{2}(j_1 + j_2 + j_3) + \left[\frac{3}{4}\pi - (j_1 f_1 + j_2 f_2 + j_3 f_3) - \mu_1 \cos^{-1} \frac{j_1^2 - j_2^2 + j_3^2}{2j_1 j_3} \right.$$

$$\left. + \mu_2 \cos^{-1} \frac{-j_1^2 + j_2^2 + j_3^2}{2j_2 j_3} \right] + \mathcal{O}(k^{-1/2}). \tag{B.11}$$

Since $\sum j_i f_i = 0$, we have

$$\cos\left[\chi + \frac{\pi}{4} - \pi(j_3 + 1)\right] = \cos\left[(j_1 + j_2 - j_3)\frac{\pi}{2} + \mu_2 \alpha_1 - \mu_1 \alpha_2\right] \tag{B.12}$$

with (see figure B1)

$$\alpha_1 := \arccos \frac{-j_1^2 + j_2^2 + j_3^2}{2j_2 j_3}, \qquad \alpha_2 := \arccos \frac{j_1^2 - j_2^2 + j_3^2}{2j_1 j_3}. \tag{B.13}$$

The remaining factor behaves as $\sqrt{\frac{j_3}{2j_3+1}} = \frac{1}{\sqrt{2}}\left(1 + \mathcal{O}(k^{-1/2})\right)$.

Collecting all the pieces we get

$$\begin{pmatrix} j_1 & j_2 & j_3 \\ \mu_1 & \mu_2 & \mu_3 \end{pmatrix} = \frac{(-1)^{j_1 - j_2 - \mu_3}}{\sqrt{2\pi A(j_1, j_2, j_3)}}$$

$$\times \cos\left[(j_1 + j_2 - j_3)\frac{\pi}{2} + \mu_2 \alpha_1 - \mu_1 \alpha_2\right](1 + \mathcal{O}(k^{-1/2})). \tag{B.14}$$

Appendix C. Free field three-point function

In the supersymmetric free field theory of two bosons and two fermions on the plane the three-point function of Neveu–Schwarz (super-)primary fields $\Phi_{\mathbf{p}}^{\text{free}}$ is very simple (see equation (3.20)). In this appendix we compute the three-point function in a radial basis $\Phi_{p,m}^{\text{free}}$, which is needed for the comparison to the limit of minimal models.

The fields $\Phi_{p,m}^{\text{free}}$ are defined as

$$\Phi_{p,m}^{\text{free}} = \sqrt{\frac{p}{2\pi}} \int d\varphi \, \Phi_{pe^{i\varphi}}^{\text{free}} e^{im\varphi}. \tag{C.1}$$

Their three-point function can therefore be expressed as

$$\langle \Phi_{p_1,m_1}^{\text{free}}(z_1, \bar{z}_1) \Phi_{p_2,m_2}^{\text{free}}(z_2, \bar{z}_2) \Phi_{p_3,m_3}^{\text{free}}(z_3, \bar{z}_3) \rangle$$

$$= \sqrt{\frac{p_1 p_2 p_3}{(2\pi)^3}} \int d\varphi_1 \, d\varphi_2 \, d\varphi_3 \, e^{im_1\varphi_1 + im_2\varphi_2 + im_3\varphi_3} \langle \Phi_{p_1 e^{i\varphi_1}}^{\text{free}}(z_1, \bar{z}_1) \Phi_{p_2 e^{i\varphi_2}}^{\text{free}}(z_2, \bar{z}_2) \Phi_{p_3 e^{i\varphi_3}}^{\text{free}}(z_3, \bar{z}_3) \rangle$$

$$= \sqrt{\frac{p_1 p_2 p_3}{(2\pi)^3}} |z_{12}|^{2(h_3 - h_1 - h_2)} |z_{23}|^{2(h_1 - h_2 - h_3)} |z_{13}|^{2(h_2 - h_1 - h_3)}$$

$$\times \int d\varphi_1 \, d\varphi_2 \, d\varphi_3 \, e^{im_1\varphi_1 + im_2\varphi_2 + im_3\varphi_3} \delta^{(2)}(p_1 e^{i\varphi_1} + p_2 e^{i\varphi_2} + p_3 e^{i\varphi_3}) \tag{C.2}$$
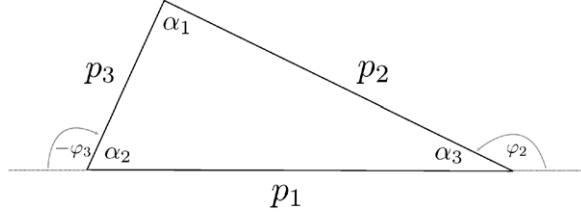
Figure C1. The triangle spanned by p_1, $p_2 e^{i\varphi_2}$ and $p_3 e^{i\varphi_3}$.

$$= \sqrt{\frac{p_1 p_2 p_3}{2\pi}} |z_{12}|^{2(h_3-h_1-h_2)} |z_{23}|^{2(h_1-h_2-h_3)} |z_{13}|^{2(h_2-h_1-h_3)}$$

$$\times \delta_{m_1+m_2+m_3} \int d\varphi_2 \, d\varphi_3 \, e^{im_2\varphi_2+im_3\varphi_3} \delta^{(2)}(p_1 + p_2 e^{i\varphi_2} + p_3 e^{i\varphi_3}). \tag{C.3}$$

We now have to evaluate the remaining integral over the angles φ_2 and φ_3. Due to the delta-distribution it only gets contributions if the two-dimensional vectors corresponding to the complex momenta p_1, $p_2 e^{i\varphi_2}$ and $p_3 e^{i\varphi_3}$ form a triangle. In particular it is zero unless the inequalities

$$|p_2 - p_3| \leqslant p_1 \leqslant p_2 + p_3 \tag{C.4}$$

are satisfied. The triangle condition arising from the delta-distribution can be formulated by the equations

$$q_1 := p_1 + p_2 \cos\varphi_2 + p_3 \cos\varphi_3 = 0, \tag{C.5}$$

$$q_2 := p_2 \sin\varphi_2 + p_3 \sin\varphi_3 = 0. \tag{C.6}$$

The angles φ_i take values in the interval $[-\pi, \pi]$. For any solution (φ_2, φ_3) there is another solution $(-\varphi_2, -\varphi_3)$ that corresponds to the triangle reflected at the side p_1. For $\varphi_2 > 0$ we have $\varphi_3 < 0$ and the relation to the angles of the triangle is given by (see figure C1)

$$\varphi_2 = \alpha_1 + \alpha_2, \qquad \varphi_3 = \alpha_2 - \pi. \tag{C.7}$$

Evaluating the integral therefore reduces to plugging in the values for φ_2 and φ_3 for the two solutions, and dividing this by the Jacobian determinant

$$\left| \det \left(\frac{\partial q_i}{\partial \varphi_j} \right)_{i,j} \right| = p_2 p_3 |\sin(\varphi_2 - \varphi_3)| = 2A(p_1, p_2, p_3), \tag{C.8}$$

where $A(p_1, p_2, p_3)$ is the area of the triangle (see equation (B.5)). We find in total

$$\langle \Phi_{p_1,m_1}^{\text{free}}(z_1, \bar{z}_1) \Phi_{p_2,m_2}^{\text{free}}(z_2, \bar{z}_2) \Phi_{p_3,m_3}^{\text{free}}(z_3, \bar{z}_3) \rangle$$

$$= \sqrt{\frac{p_1 p_2 p_3}{2\pi}} |z_{12}|^{2(h_3-h_1-h_2)} |z_{23}|^{2(h_1-h_2-h_3)} |z_{13}|^{2(h_2-h_1-h_3)}$$

$$\times \delta_{m_1+m_2+m_3} \frac{\cos(m_2\alpha_1 - m_1\alpha_2 + \pi(m_1 + m_2))}{A(p_1, p_2, p_3)}. \tag{C.9}$$

References

[1] Runkel I and Watts G 2001 A nonrational CFT with $c = 1$ as a limit of minimal models *J. High Energy Phys.* JHEP09(2001)006 (arXiv:hep-th/0107118)

[2] Graham K, Runkel I and Watts G 2001 Minimal model boundary flows and $c = 1$ CFT *Nucl. Phys.* B **608** 527 (arXiv:hep-th/0101187)

[3] Roggenkamp D and Wendland K 2004 Limits and degenerations of unitary conformal field theories *Commun. Math. Phys.* **251** 589 (arXiv:hep-th/0308143)

[4] Fredenhagen S and Schomerus V 2005 Boundary Liouville theory at $c = 1$ *J. High Energy Phys.* JHEP05(2005)025 (arXiv:hep-th/0409256)

[5] Fredenhagen S and Wellig D 2007 A common limit of super Liouville theory and minimal models *J. High Energy Phys.* JHEP09(2007)098 (arXiv:0706.1650)

[6] Roggenkamp D and Wendland K 2008 Decoding the geometry of conformal field theories *Bulg. J. Phys.* **35** 139 (arXiv:0803.0657)

[7] Fredenhagen S 2011 Boundary conditions in Toda theories and minimal models *J. High Energy Phys.* JHEP02(2011)052 (arXiv:1012.0485)

[8] Fredenhagen S, Restuccia C and Sun R 2012 The limit of $N = (2, 2)$ superconformal minimal models *J. High Energy Phys.* JHEP10(2012)141 (arXiv:1204.0446)

[9] Zamolodchikov A 1986 Irreversibility of the flux of the renormalization group in a 2D field theory *JETP Lett.* **43** 730

[10] Kutasov D 1989 Geometry on the space of conformal field theories and contact terms *Phys. Lett.* B **220** 153

[11] Douglas M R 2010 Spaces of quantum field theories arXiv:1005.2779

[12] Maldacena J M, Moore G W and Seiberg N 2001 Geometrical interpretation of D-branes in gauged WZW models *J. High Energy Phys.* JHEP07(2001)046 (arXiv:hep-th/0105038)

[13] Andrews G E, Askey R and Roy R 1999 *Special Functions (Encyclopedia of Mathematics and Its Applications vol 71)* (Cambridge: Cambridge University Press)

[14] Blumenhagen R, Lüst D and Theisen S 2013 *Basic Concepts of String Theory* (Heidelberg: Springer)

[15] Mussardo G, Sotkov G and Stanishkov M 1989 $N = 2$ superconformal minimal models *Int. J. Mod. Phys.* A **4** 1135

[16] Zamolodchikov A B and Fateev V A 1986 Operator algebra and correlation functions in the two-dimensional Wess–Zumino SU(2)×SU(2) chiral model *Sov. J. Nucl. Phys.* **43** 657

[17] Dotsenko V 1991 Solving the SU(2) conformal field theory with the Wakimoto free field representation *Nucl. Phys.* B **358** 547

[18] Ooguri H, Oz Y and Yin Z 1996 D-branes on Calabi–Yau spaces and their mirrors *Nucl. Phys.* B **477** 407 (arXiv:hep-th/9606112)

[19] Hori K, Iqbal A and Vafa C 2000 D-branes and mirror symmetry arXiv:hep-th/0005247

[20] Cardy J L 1989 Boundary conditions, fusion rules and the Verlinde formula *Nucl. Phys.* B **324** 581

[21] Fredenhagen S 2003 Organizing boundary RG flows *Nucl. Phys.* B **660** 436 (arXiv:hep-th/0301229)

[22] Abouelsaood A, Callan J, Curtis G, Nappi C R and Yost S A 1987 Open strings in background gauge fields *Nucl. Phys.* B **280** 599

[23] Di Vecchia P and Liccardo A 1999 D-branes in string theory: II arXiv:hep-th/9912275

[24] Gaberdiel M R and Klemm H 2004 $N = 2$ superconformal boundary states for free bosons and fermions *Nucl. Phys.* B **693** 281 (arXiv:hep-th/0404062)

[25] Gaberdiel M R and Suchanek P 2012 Limits of minimal models and continuous orbifolds *J. High Energy Phys.* JHEP03(2012)104 (arXiv:1112.1708)

[26] Billo M, Craps B and Roose F 2001 Orbifold boundary states from Cardy's condition *J. High Energy Phys.* JHEP01(2001)038 (arXiv:hep-th/0011060)

[27] Kazama Y and Suzuki H 1989 New $N = 2$ superconformal field theories and superstring compactification *Nucl. Phys.* B **321** 232

[28] Gaberdiel M R and Gopakumar R 2011 An AdS$_3$ dual for minimal model CFTs *Phys. Rev.* D **83** 066007 (arXiv:1011.2986)

[29] Gaberdiel M R and Gopakumar R 2012 Minimal model holography arXiv:1207.6697

[30] Creutzig T, Hikida Y and Rønne P B 2012 Higher spin AdS$_3$ supergravity and its dual CFT *J. High Energy Phys.* JHEP02(2012)109 (arXiv:1111.2139)

[31] Candu C and Gaberdiel M R 2012 Supersymmetric holography on AdS$_3$ arXiv:1203.1939

[32] Hanaki K and Peng C 2012 Symmetries of holographic super-minimal models arXiv:1203.5768

[33] Ahn C 2012 The large N 't Hooft limit of Kazama–Suzuki model *J. High Energy Phys.* JHEP08(2012)47 (arXiv:1206.0054)

[34] Candu C and Gaberdiel M R 2012 Duality in $N = 2$ minimal model holography arXiv:1207.6646

[35] Klemm H 2004 Embedding diagrams of the $N = 2$ superconformal algebra under spectral flow *Int. J. Mod. Phys.* A **19** 5263 (arXiv:hep-th/0306073)

[36] Kiritsis E 1988 Character formulae and the structure of the representations of the $N = 1$, $N = 2$ superconformal algebras *Int. J. Mod. Phys.* A **3** 1871

[37] Eholzer W and Gaberdiel M 1997 Unitarity of rational $N = 2$ superconformal theories *Commun. Math. Phys.* **186** 61 (arXiv:hep-th/9601163)

[38] Lerche W, Vafa C and Warner N P 1989 Chiral rings in $N = 2$ superconformal theories *Nucl. Phys.* B **324** 427

[39] Ravanini F and Yang S-K 1987 Modular invariance in $N = 2$ superconformal field theories *Phys. Lett.* B **195** 202

[40] Reinsch M W and Morehead J J 1999 Asymptotics of Clebsch–Gordan coefficients *J. Math. Phys.* **40** 4782 (arXiv:math-ph/9906007)

[41] Ponzano G and Regge T 1968 Semiclassical limit of Racah coefficients *Spectroscopic and Group Theoretical Methods in Physics* ed F Bloch (Amsterdam: North-Holland) pp 1–58